Statistical mechanics of hydrodynamic lattice gases

by

Anatoly Malevanets

A thesis submitted in conformity with the requirements
for the degree of Doctor of Philisophy
Graduate Department of Chemistry
University of Toronto

ABSTRACT

In this thesis we present a model for fluid dynamics computations. The model combines a stochastic propagation scheme with special collision rules. We consider a class of collision rules with local mass, momentum and energy conservation laws. We derive the Boltzmann equation for the model and show that the Boltzmann H-theorem holds. By carrying out a Chapman-Enskog analysis we deduce that the macroscopic evolution of the system is governed by the Navier-Stokes equations. In the linear response approximation we derive Green-Kubo formulae for the discrete system and show that the Onsager reciprocal relations are valid for the model without microscopic reversibility. We derive expressions for the transport coefficients in terms of autocorrelation functions. Numerical experiments performed on the model support the theoretical analysis and demonstrate that the model provides a stable simulation method for turbulent hydrodynamic flows.

CONTENTS

1. Introduction 1

2. Lattice gas model 6

2.1 Notations 7

2.2 Algorithmic description 10

2.2.1 Particles and sites 11

2.2.2 Streaming transformation 12

2.2.3 Collision transformation 14

2.3 Streaming operator 16

2.3.1 Transition model 18

2.4 Elementary properties of collision operator 20

2.5 Boltzmann equation 25

2.6 Boltzmann H-theorem 26

3. Hydrodynamic equations and transport coefficients 31

3.1 Chapman-Enskog asymptotic expansion 31

3.2 Navier-Stokes equation 33

4. Green-Kubo formulae and computation of transport coefficients . 41

4.1 Green-Kubo formulae 41

4.1.1 Projected dynamics 42

4.1.2 **k**-dependence of the operator $\mathcal{P}(\mathcal{W}-\hat{1})$ 44

4.1.3 Symmetry of time-correlation function 45

4.1.4 Evolution of the locally conserved quantities 47

4.2 Hydrodynamic equations in Green-Kubo formalism 50

4.3 Computation of the transport coefficients 53

4.3.1 Self-diffusion coefficient 54

4.3.2 Viscosity coefficient 56

5. Numerical study of the lattice gas model 61

5.1 Equilibrium properties 61

5.2 Simulations of fluid dynamics 68

6. Conclusion 74

LIST OF FIGURES

3.1 Kinematic viscosity for different collision models at $T^* = 1$. . . 37

3.2 Pictorial representation of the streaming transformation in the stochastic model. 38

5.1 Numerical and theoretical energy probability distribution densities. The solid line shows the Maxwell energy profile. The dotted line is obtained from numerical simulations. 62

5.2 A test of equation of state of the lattice gas model. 63

5.3 Velocity-velocity and stress-stress normalized time correlation functions for the collision model with an orthogonal scattering of the colliding particles. 64

5.4 Velocity-velocity and stress-stress normalized time correlation functions for the collision model with a random scattering of the colliding particles. 65

5.5 Simulation of two dimensional von Karman street. 72

5.6 Development of a turbulent boundary layer for a high Reynolds number flow. 73

1. INTRODUCTION

Over the past few years lattice gas models have attracted the attention of researchers in various disciplines.[1-4] In 1986, Frisch, Hasslacher and Pomeau (FHP) introduced a model[5] that in the long-time, large-scale limit leads to the Navier-Stokes equations. In two dimensions the model consists of a set of particles on the triangular lattice. The particles propagate among lattice vertices with unit velocities and interact with each other according to some artificial local collision rules that satisfy particle number and momentum conservation laws. This model demonstrated that the complexity of hydrodynamics may be obtained from a drastically simplified version of molecular dynamics. Since the introduction of the original FHP model a number of extensions of the model have been developed which have allowed one to investigate the properties of complex systems built on simplified microscopic dynamics. On the computational side, it has been shown that lattice gas models provide stable simulation schemes that are highly parallelizable and are efficiently realized either on conventional parallel and vector computers or specifically designed architectures.[6]

The atomistic nature of matter suggests that many dynamical processes in

the physical and biological sciences are good candidates for the application of such schemes. The lattice gas models of hydrodynamic flows inspired a variety of other applications; for example, these models have been successfully applied to simulations of microemulsion formation,[7] phase separation[8] and reaction-diffusion processes.[9] Lattice gas models may be used to carry out simulations of large or complex systems where full molecular dynamics is not feasible. Since lattice gas models utilize a simplified description of phase space with disrete positions and velocities and employ an exclusion principle which restricts the number of particles at a site on the lattice, lattice gas dynamics has some peculiar features: the equilibrium distribution is Fermi-Dirac and energy relaxation processes cannot be treated since there is only a single speed in the model.

Other schemes have been devised to overcome some of these limitations. There exist multiple-velocity lattice-gas and Boltzmann models;[10] these models extend the phase space by considering a finite, but sometimes large, collection of particle velocities on the lattice. There are also stochastic simulation methods for the Boltzmann equation[11] that provide approximate molecular dynamics schemes with continuous velocities. There have also been extensive developments of lattice Boltzmann methods[12,13] which retain the discreteness of the lattice but work at the level of the real-valued particle distribution. While powerful, this method lacks the inherent stability of lattice gas methods.

The motivation behind the construction of the present lattice gas model was the desire to combine the stability of the lattice gas automaton and the Maxwellian character of the colliding molecules. In the thesis we propose a stochastic lattice gas model with an internal continuous vector parameter. This vector parameter may be identified with the particle velocity. A major obstacle is the discreteness of the underlying lattice, which makes it impossible to formulate a deterministic streaming rule for continuous velocities. Thus, we are forced to abandon microscopic reversibility which is intrinsic to the deterministic rule. We introduce a stochastic transition scheme and show that in a certain limit the behaviour of the system is described by the hydrodynamic equations. These two features, the existence of the vector parameter and the stochastic particle propagation, distinguish the present model from conventional lattice gas models.[14] Some features of the proposed model make it similar to the Bird scheme[11] for the Boltzmann equation simulations.

Using the semi-detailed balance property of the system, we have established the Boltzmann H-theorem for the reduced particle probability distribution. By carrying out a Chapman-Enskog analysis on the lattice gas model, we have shown that the evolution of the locally conserved fields is described by the Navier-Stokes equations. Further investigations of the system have shown that while microscopic reversibility is absent from the system one may still show that processes with inverted velocities are symmetric in a certain sense and Onsager reciprocal relations may be established for the model. Using projection operator techniques[15] we have derived Green-Kubo formulae in

the linear response regime and obtained autocorrelation function expressions for the transport coefficients. The autocorrelation expressions have a special form due to the discrete character of the time evolution.

We applied the lattice gas model to simulations of fluid flow with moderate Reynolds numbers. The results of the numerical experiments established the utility of the method. We observed the von Karman street type of flow past a cylinder at the expected Reynolds numbers. At lower values of the Reynolds number we observed a steady double vortex and a steady laminar flow past the cylinder.

The thesis is organized as follows. We first present in Chapter 2 the operational description of the lattice gas model. Later in this section we give an alternative formulation in terms of the evolution of the probability density.

In Chapter 3 we solve the evolution equation in the Boltzmann approximation using the Chapman-Enskog procedure. We present the system of evolution equations for the collisional invariants and show how the Navier-Stokes equations are obtained.

In Chapter 4 we develop the Green-Kubo formalism for the lattice gas system and derive expressions for the transport coefficients in terms of sums of the corresponding "force-force" autocorrelation functions. Based on these formulae, we give an alternative derivation of the expressions for the transport coefficients in the Boltzmann approximation.

We test the theoretical predictions against numerical simulations of the model

in Chapter 5. In this chapter we also present applications of the lattice gas model to simulations of fluid flow. We demonstrate that the lattice gas model is able to reproduce the main features of a flow with high Reynolds numbers. Finally, the conclusions are summarized in Chapter 6.

2. LATTICE GAS MODEL

In this chapter we shall build a general framework for the efficient description of stochastic lattice gas models. A major difficulty lies in differences between the algorithm of the proposed computational scheme and mathematical tools used for the model analysis. On the algorithmic level one works with random variables and the evolution of the system results from the transformations of such random variables. On the other hand, microscopic behaviour is more conveniently described in terms of expectations of the microscopic quantities of interest. We provide an interface between the algorithmic and phase space pictures of such dynamics. In the course of the work we establish links between the microscopic and macroscopic descriptions and further illuminate the above-mentioned duality.

We further investigate analytical properties of the collision and propagation operators. We prove a variant of the Boltzmann H-theorem and prove that a Maxwellian distribution is a stationary solution. A method for computing collision integral will be presented and values of transport coefficients will be evaluated. Interaction with external fields and boundary collisions will be dealt with in the later chapters.

2.1 Notations

In this work we attempt to use notations for different sorts of objects consistently. We use doublelined capital(Blackboard Bold, e.g. $\mathbb{L}, \mathbb{V}$) letters for function spaces, such as phase space, coordinate space and so on. Script letters (e.g. $\mathcal{C}, \mathcal{D}$) are used mainly for operators. Examples are the collision and streaming operators. We denote vector variables with bold letters (e.g. $\mathbf{v} = \{v_x, v_y, v_z\}$). A collection of variables of the same type is symbolized by a capital letter of the same variable (e.g. $\mathbf{V} = \{\mathbf{v}_1, \ldots, \mathbf{v}_n\}, I = \{i_1, i_2, i_3\}$). We emphasize the random character of the dynamical variables by using Greek letters e.g. ξ, ζ. We often omit an argument, an event in the probability space, from random variables. With sans serif letters we denote gross quantities on a lattice site such as the total number of particles n and the velocity of the centre of mass V. When there is an ambiguity in the choice of notation, we shall be guided by esthetic principles.

Functions defined on the following spaces will play a major role in this thesis:

$\mathbb{L}$ - a set of lattice nodes,

$\mathbb{V}$ - a vector space of particle velocities,

$\mathbb{Q} = (\mathbb{L} \otimes \mathbb{V})^n$ - phase space of n particles,

$\mathbb{S} = \bigoplus_{i=0}^{\infty} \mathbb{V}^i$ - collision space.

$\mathbb{L}$ is a discrete coordinate space, the nodes of which comprise a regular lattice.

Primarily we consider cubic lattices in three dimensions and square lattices in two dimensions. In the model considered below restrictions on lattice symmetry are less severe than in the classic FHP[14] model. As we show later in detail, symmetry of the second rank pressure tensor arises from symmetry of the local particle probability distribution rather than from the symmetry of the underlying lattice.

The major novel feature of the present lattice gas model is the introduction of a continuous internal vector parameter $\mathbf{v} \in \mathbb{V}$ which later will be associated with the particle velocity. Current lattice-gas models possess a discrete set of velocities, partially imposed by the underlying lattice $\mathbb{L}$. Collisions of the particles with small integer velocities lead to a limited number of outcomes and may be efficiently realized using integer arithmetic and employing update tables. However, an increase in number of velocities leads to an exponential increase in the size of update table, thus, seriously hindering performance. Of course performance is only of secondary importance in the study of lattice-gas models, which constitute new media for the investigation of non-equilibrium phenomena in physics and chemistry. In the present model the space of possible velocities $\mathbb{V}$ is $\mathbb{R}^3$ in three dimensions and $\mathbb{R}^2$ for two dimensional lattices. Occasionally, for convenience, in two dimensions we associate $\mathbb{V}$ with the vector space of complex numbers $\mathbb{C}$.

The phase space $\mathbb{Q} = \mathbb{L} \otimes \mathbb{V}$ is used in two different contexts. As a domain of definition of mapping $f : \mathbb{Q} \to \mathbb{R}^+$, it used in dealing with reduced probability

distributions and, on the algorithmic level, it defines the position and state of a particle. In the description of chemical transformations, not considered in this thesis, $\mathbb{Q}$ can be used for states of molecules with additional internal degrees of freedom. In this case it acquires the meaning $\mathbb{Q} = \mathbb{L} \otimes \mathbb{V} \otimes \mathbb{I}$.

The space $\mathbb{S}$ naturally arises in the description of collisions with different numbers of particles. Each collision is described by the number of colliding particles and their internal properties. For particles of the same species without internal degrees of freedom it expressed functionally as a direct sum of $\mathbb{V}^n$ or $\mathbb{S} = \bigoplus_{i=0}^{\infty} \mathbb{V}^i$. For convenience at this point we introduce several useful functionals on this space. A mapping $\mathsf{n} : \mathbb{S} \to \mathbb{Z}^+$ makes a correspondence between a collision and the number of the colliding particles. When confusion is unlikely we omit the argument of the functional n. Other important quantities are the average velocity and the sum of square norms of the velocities. For non-zero particle collisions, $s \in \mathbb{S}$, these quantities are defined as:

$$\mathsf{M}(s) = \sum_{i=1}^{\mathsf{n}} m_i,$$

$$\mathsf{V}(s) = \frac{1}{\mathsf{M}} \sum_{i=1}^{\mathsf{n}} m_i \mathbf{v}_i,$$

$$\mathsf{E}(s) = \frac{1}{2} \sum_{i=1}^{\mathsf{n}} m_i \|\mathbf{v}_i\|^2,$$

where m_i are the masses of the colliding particles.

A system state can be specified in two different ways. A knowledge of positions and internal degrees of freedom, including velocity, for each particle

fully specifies the system. Alternatively, one may define system state in terms of the distribution of particles on a lattice by assigning to every site $\mathbf{l} \in \mathbb{L}$ a collision state $c \in \mathbb{S}$. We use both descriptions, the former for analyzing properties of the streaming operator and the later for studying collisions.

2.2 Algorithmic description

In this section we give a detailed description of the algorithm used in numerical simulations. Validation of the computation scheme is given in later sections. However, we sometimes refer to these results in qualitative comparisons of different approaches.

The lattice-gas model involves consecutive application of the streaming and collision transformations on the system. We consider the particular case where the streaming and collision transformations act independently on the sets of particles and sites respectively.

The particles possess internal variables which constitute an essential feature of the model. In the model the internal variables change only in the course of collisions with the other particles and the change is further constrained to satisfy a set of rules – conservation laws. The conservation laws closely resemble conservation of energy and momentum and we refer to these laws by those names.

2.2.1 Particles and sites

We consider a system consisting of a set of particles on a regular lattice. Sites are a set of the lattice discrete coordinates. Particles may be identical or may belong to different classes and are characterized by their position, mass, momentum, energy (and possibly other internal parameters). There is no restriction on the number of particles per site. The position of the particle is given by its discrete coordinates on the lattice and is changed only during the streaming transformation. The other attributes of the particle may be changed only during collisions with the other particles or external fields. The masses of particles of the same type are taken to be the same and are conserved during evolution. In this case mass and particle number densities describe the same quantity. The momentum is a vector variable used to define particle streaming and is closely related to the particle velocity.

The formal description of the particle structure is presented in the following block-scheme:

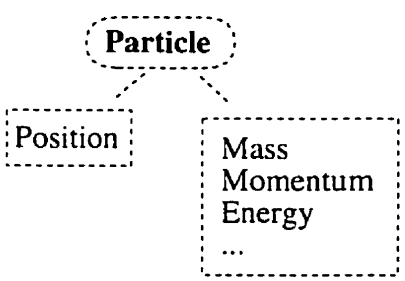

In the discrete space we may separate particles into groups according to their positions. The collision transformation acts on such groups independently and, in general, requires information on all attributes of the residing particles.

It is natural to assume that collisions satisfying conservation laws may be built from a knowledge of the conserved quantities only. Such models are especially convenient for computations. In this case a site consists of total energy, momentum and mass depicted in the following scheme:

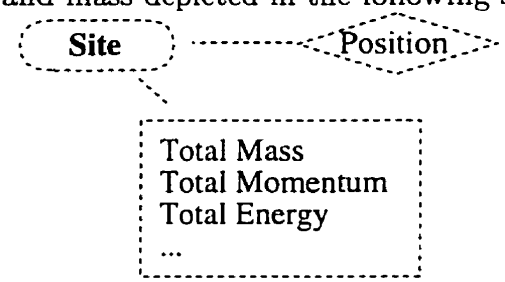

2.2.2 *Streaming transformation*

We call any operation on the system that changes the positions of the particles a streaming operator. The streaming transformation is defined to act solely on the particle velocities (velocity = momentum/mass) and does not affect the internal parameters of the particles. Consider a particle with velocity $\mathbf{v}$,

$$\mathbf{v} = \sum_i v_i \mathbf{e}_i,$$

where $\mathbf{e}_i$ are generators of the regular lattice. We shall discuss a construction of such a representation later.

Propagation of a particle is defined by integer random numbers η_i with the following property:

$$E\big(\eta_i(v_i)\big) = v_i.$$

The above formula relates the particle momentum to the particle propagation velocity. In this case propagation of the particle during one streaming step is given by:

$$\mathbf{e} = \sum_i \eta_i(v_i)\mathbf{e}_i$$

and we further restrict ourselves to the case of identically distributed random numbers η_i for all i for reasons of symmetry.

One choice of random numbers has the following distribution:

$$P\big(\eta(v) = n\big) = \begin{cases} \{v\} & n = [v] + 1, \\ 1 - \{v\} & n = [v], \\ 0 & \text{else}, \end{cases} \tag{2.1}$$

where $\{v\}$ and $[v]$ are fractional and integer parts of v, respectively, and the following identity holds:

$$\{v\} + [v] = v.$$

The probability distribution (2.1) is obtained by comparison of fractional part $\{v\}$ with a uniformly distributed random variable ξ on $[0, 1]$. Computations show that

$$P\big(\xi > \{v\}\big) = P\big(\eta(v) = [v]\big),$$
$$P\big(\xi < \{v\}\big) = P\big(\eta(v) = [v] + 1\big).$$

We show that this choice of random streaming is optimal, namely, it gives the smallest streaming contribution to the dissipative effects.

Another convenient choice for the description of streaming may be built on Poisson distributed random numbers:

$$P(\eta(v) = n) = \frac{v^n}{n!}e^{-v} \quad , n \geq 0.$$

A disadvantage of this choice is the lack of Galilean invariance of the resulting hydrodynamics equation. It also gives a large dissipative contribution for large velocities.

The above algorithm for particle transfer is implemented as an update of position fields for all particles independently.

2.2.3 *Collision transformation*

A collision transformation is a process that acts on group of particles at a site but does not change their positions. Very complex collision transformations can be implemented on the set of particles at a site. However, for most collision schemes the change in internal variables depends on a fixed number of collision parameters.

We experimented with a class of such schemes which depends only on gross quantities such as total momentum, energy and mass and an additional random rotation matrix. This class of collision rules still provides for very rich phenomenology. The schemes are based on the fact that rotations of the velocities in the frame moving with the velocity of the center of mass does

not change the excess of the kinetic energy and thus the total energy.[1]

We implemented collision transformations as a three-step update. On the first step, for each particle, we incremented total mass, energy and momentum at the site corresponding to the particle position by those values of the particle. On the second step we computed velocity of the center of mass V and a random rotation matrix σ at each site. This update step is performed on the set of sites. Lastly, for each particle we updated velocities according to the formula:

$$\mathbf{v}' = \mathsf{V} + \sigma(\mathbf{v} - \mathsf{V}).$$

Computations show that total energy and momentum are conserved in the above operation. The values of the transport coefficients depend on the details of the collision model and, in the case of a monatomic ideal gas, are defined by choices of collision matrices. Two such choices are considered in this work. The first class of collision models is given by a set of random rotations in $O(d)$ with uniform density. The second choice is given by a set of random rotations $\{\sigma_i\}$ that transform a vector V into an orthogonal vector: $(\mathsf{V}^T, \sigma_i \mathsf{V}) = 0$. The second choice yields the smallest value of the shear viscosity coefficient in the Boltzmann approximation.

In simulations, as random rotations we used a small array of predefined rotations. Numerical experiments did not detect any effects arising from the

[1] We consider systems with quadratic dependence of the kinetic energy of a particle on the momentum of the particle.

non-random character of these rotations. We attribute this observation to the immense complexity of the system under consideration.

2.3 Streaming operator

The streaming operator acts independently on all particles in the system. We consider a class of translationally invariant streaming operators. In terms of the reduced probability distribution P_1, $P_1 : \mathbb{Q} \to \mathbb{R}$ it is expressed as

$$\mathcal{S}P_1(\mathbf{l}, \mathbf{v}) = \sum_{\mathbf{r} \in \mathbb{L}} W(\mathbf{r}, \mathbf{v}) P_1(\mathbf{l} - \mathbf{r}, \mathbf{v}). \tag{2.2}$$

The above formula is conveniently rewritten with the use of the cumulant expansion for Markov processes specified by transition probabilities W. One may verify the following identity by consecutive application of differentiation to both sides of the equation

$$\sum_{\mathbf{r} \in \mathbb{L}} W(\mathbf{r}, \mathbf{v}) e^{\mathbf{r} \cdot \mathbf{k}} = \sum_{n=0}^{\infty} \frac{\mathsf{m}_n}{n!} \odot \mathbf{k}^n = \exp\Big(\sum_{n=1}^{\infty} \frac{\boldsymbol{\kappa}_n}{n!} \odot \mathbf{k}^n\Big), \tag{2.3}$$

where $\odot$ denotes the tensor contraction, m are the moments, $\boldsymbol{\kappa}$, the cumulants and the second identity serves as a definition of the cumulant expansion. If we use formal expressions for translation operators in space and in time as $f(\mathbf{r} + \mathbf{l}) = e^{\mathbf{l} \cdot \boldsymbol{\nabla}} f(\mathbf{r})$ and $f(t + 1) = e^{\frac{\partial}{\partial t}} f(t)$, respectively, we may rewrite (2.2) with the use of (2.3) in terms of a cumulant expansion in terms of powers of $\boldsymbol{\nabla}$:

$$\mathcal{S} = \exp\Big(\sum_{n=1}^{\infty} \frac{\boldsymbol{\kappa}_n(\mathbf{v})}{n!} \odot [-\boldsymbol{\nabla}]^n\Big). \tag{2.4}$$

We apply the formal expression (2.4) to a system of non-interacting particles. Evolution in discrete time is expressed using finite-time translation in the exponential form (2.4):

$$P_1(\mathbf{l}, \mathbf{v}, t+1) = \mathcal{S}P_1(\mathbf{l}, \mathbf{v}, t) = \sum_{\mathbf{r}\in\mathbb{L}} W(\mathbf{r}, \mathbf{v}) P_1(\mathbf{l} - \mathbf{r}, \mathbf{v}, t), \tag{2.5}$$

or

$$\exp\left(\frac{\partial}{\partial t}\right) P_1(\mathbf{l}, \mathbf{v}, t) - \exp\left(\sum_{n=1}^{\infty} \frac{\boldsymbol{\kappa}_n(\mathbf{v})}{n!} \odot [-\boldsymbol{\nabla}]^n\right) P_1(\mathbf{l}, \mathbf{v}, t) = 0, \tag{2.6}$$

which may be expressed as

$$\mathcal{S}\left[\int_0^1 e^{\tau\mathcal{X}} d\tau\right] \mathcal{X} P_1(\mathbf{l}, \mathbf{v}, t) = 0, \tag{2.7}$$

where

$$\mathcal{X} = \frac{\partial}{\partial t} - \sum_{n=1}^{\infty} \frac{\boldsymbol{\kappa}_n(\mathbf{v})}{n!} \odot [-\boldsymbol{\nabla}]^n. \tag{2.8}$$

We may establish a connection between the continuous vector parameter $\mathbf{v}$ and the particle velocity by imposing the requirement

$$\boldsymbol{\kappa}_1(\mathbf{v}) = \langle \mathbf{r} \rangle_W = -\mathbf{v}.$$

Below we will use these two notations for the quantity interchangeably. Evolution of the probability density in the long time – long distance limit is given by the following Fokker-Planck equation:

$$\frac{\partial}{\partial t} P_1 + \mathbf{v} \cdot \boldsymbol{\nabla} P_1 = \frac{1}{2} \langle\langle r_i r_j \rangle\rangle_W \nabla_i \nabla_j P_1. \tag{2.9}$$

2.3.1 Transition model

If models employing independent propagations along coordinate axes are used, cross-cumulants vanish. A particularly simple scheme is to translate a particle in the x-direction during a unit time by $[v_x]$ with probability $1-\{v_x\}$ and by $[v_x]+1$ with probability $\{v_x\}$. By $[x]$ we denote the largest integer not exceeding x and by $\{x\}$ the fractional part of x. These quantities are related to each other by $\{x\}+[x]=x$.

Transition probabilities satisfy the normalization condition,

$$(1-\{v_x\})+\{v_x\}=1,$$

and we verify that the average velocity of a particle is indeed v_x:

$$\langle l_x\rangle = (1-\{v_x\})[v_x]+\{v_x\}([v_x]+1)=v_x.$$

In the one dimensional case the moment of nth power is given by the expression:

$$\mathsf{m}_n = (1-\{v_x\})[v_x]^n+\{v_x\}([v_x]+1)^n,$$

and from recurrence relations for the second and third cumulants in terms of moments we have:

$$\kappa_2(\mathbf{v}) = \mathsf{m}_2-\mathsf{m}_1^2$$

$$\kappa_3(\mathbf{v}) = \mathsf{m}_3-3\mathsf{m}_1\mathsf{m}_2+2\mathsf{m}_1^3,$$

from which we derive the following formulae:

$$\kappa_2(\mathbf{v}) = \{v_x\}(1 - \{v_x\})$$
$$\kappa_3(\mathbf{v}) = (\{v_x\} - 1)(2\{v_x\} - 1)\{v_x\}.$$

Averages of products of smooth functions with the second cumulant over a Maxwell distribution play an important role in the subsequent discussion. In this context it is convenient to appeal to the following representation of the second cumulant $\{v_x\}(1 - \{v_x\})$ as a Fourier series[16] :

$$\{v_x\}(1 - \{v_x\}) = \frac{1}{6} - \sum_{k=1}^{\infty} \frac{\cos(2\pi k v_x)}{\pi^2 k^2}. \tag{2.10}$$

In the above expression we replaced the argument in the cosine by noting that $\{v_x\}$ is a periodic function and $\cos(2\pi k\{v_x\}) = \cos(2\pi k v_x)$ for any integer k. Computations of averages over polynomial functions become straightforward and, as an example, the average of unity is given by:

$$\langle \kappa_2(v_x) f_0 \rangle = \frac{1}{6} - \sum_{k=1}^{\infty} \frac{\cos(2\pi k u_x) e^{-\frac{k^2\pi^2 T}{m}}}{\pi^2 k^2}. \tag{2.11}$$

For the parameter values used in the model the sum quickly converges and the second and higher terms of the expansion are negligibly small. Thus, for a value of the ratio $\frac{T}{m} = 1$, the second and third terms are 0.54×10^{-9} and 0.26×10^{-35}, respectively. We are justified in keeping only the first term, $\frac{1}{6}$. The behaviour of integrals of other conserved quantities is similar and for all collision invariants ι^α we approximate the diffusive term by the Laplace

operator:

$$\frac{1}{2}\nabla^2 : \langle \iota^\alpha \kappa_2(\mathbf{v}) f_0 \rangle = D\Delta \langle \iota^\alpha \rangle_{\mathsf{m}}, \tag{2.12}$$

with $D = \frac{1}{12}$.

2.4 Elementary properties of collision operator

The collision transformation acts on lattice sites independently and, thus, is formally expressed as a direct product of $\|\mathbb{L}\|$ elementary collision operators on $\mathbb{S}$.

Properties of a lattice gas model are conveniently described in terms of dynamical variables associated with macroscopic quantities. Below we give expressions for the density, momentum and kinetic energy as functions of constitutive particles. For a system with N particles we have:

$$\rho(\mathbf{l}) = \sum_{i=1}^{N} m_i \delta(\mathbf{l} - \boldsymbol{\xi}_i), \tag{2.13a}$$

$$\boldsymbol{\mu}(\mathbf{l}) = \sum_{i=1}^{N} m_i \boldsymbol{\zeta}_i \delta(\mathbf{l} - \boldsymbol{\xi}_i), \tag{2.13b}$$

$$\varepsilon(\mathbf{l}) = \sum_{i=1}^{N} \frac{1}{2} m_i \|\boldsymbol{\zeta}_i\|^2 \delta(\mathbf{l} - \boldsymbol{\xi}_i), \tag{2.13c}$$

where $\boldsymbol{\zeta}_i$ and $\boldsymbol{\xi}_i$ are, respectively, the velocity and position of the ith particle.

A dual representation of dynamical variables, which depends only on the particle distribution among sites, is built as follows. Any dynamical variable

ϕ corresponding to a function f on $\mathbb{S} = \bigoplus_{i=0}^{\infty} \mathbb{V}^i$ can be represented by the following sum:

$$\phi(S,1) = \frac{1}{N!} \sum_{\{\pi\}} \binom{N}{n} \sum_{n} f_n(\vartheta_{\pi(1)}, \ldots, \vartheta_{\pi(n)}) \times \\ \times \prod_{i=1}^{n} \delta(1 - \xi_{\pi(i)}) \prod_{i=n+1}^{N} [1 - \delta(1 - \xi_{\pi(i)})], \quad (2.14)$$

where $\{\pi\}$ is a set of permutations of N particles, S is the state of site 1 and ϑ_i denotes the internal state of ith particle, which includes particle velocity ζ_i.

For additive functions f such as number of particles and total momentum there is a connection between representations (2.14) and (2.13a)-(2.13c). Let us consider the following identity:

$$\prod_{i=1}^{N} [1 - \delta(1 - \xi_i) + e^{uf(\vartheta_i)} \delta(1 - \xi_i)] = \frac{1}{(N-n)!n!} \sum_{\{\pi\}} \times \\ \times \sum_{n} \exp\left(u \sum_{i=1}^{n} f(\vartheta_{\pi(i)})\right) \prod_{i=1}^{n} \delta(1 - \xi_{\pi(i)}) \prod_{i=n+1}^{N} [1 - \delta(1 - \xi_{\pi(i)})],$$

and differentiation of the left and right hand sides of the above identity with respect to u at $u = 0$ establishes the relation between site and particle dynamical variables.

From (2.14) we obtain the particle number distribution among the sites in the Boltzmann approximation. The probability to have n particles at a site

is given by:

$$P(\mathsf{n}=n,\mathbf{l}) = \frac{N!}{n!(N-n)!}\left\langle \prod_{i=1}^{n}\delta(\mathbf{l}-\boldsymbol{\xi}_{\pi(i)}) \prod_{i=n+1}^{N}\left[1-\delta(\mathbf{l}-\boldsymbol{\xi}_{\pi(i)})\right]\right\rangle =$$

$$= \frac{N!}{n!(N-n)!}\big(P(\boldsymbol{\xi}=\mathbf{l})\big)^{n}\big(1-P(\boldsymbol{\xi}=\mathbf{l})\big)^{N-n} \approx \frac{\big[NP(\boldsymbol{\xi}=\mathbf{l})\big]^{n}}{n!}e^{-NP(\boldsymbol{\xi}=\mathbf{l})}$$

when $NP(\boldsymbol{\xi}=\mathbf{l}) \sim O(1)$ and $N \gg 1$ and, thus, particles are distributed according to the Poisson distribution law.

For the ideal monatomic lattice gas model discussed in Sec. 2.2.3 dynamical variables change in collisions according to the following rule:

$$\boldsymbol{\zeta}_i' = \mathsf{V} + \sigma\big[\boldsymbol{\zeta}_i - \mathsf{V}\big]. \tag{2.15}$$

We see that total momentum and energy are conserved in the collisions:

$$\mathsf{MV}' = \sum_{i=1}^{\mathsf{n}} m_i\boldsymbol{\zeta}_i' = \mathsf{MV} + \sigma\sum_{i=1}^{\mathsf{n}} m_i\big[\boldsymbol{\zeta}_i - \mathsf{V}\big] = \mathsf{MV},$$

$$\sum_{i=1}^{\mathsf{n}} m_i\|\boldsymbol{\zeta}_i'\|^2 = \mathsf{M}\|\mathsf{V}'\|^2 + \sum_{i=1}^{\mathsf{n}} m_i\|\boldsymbol{\zeta}_i' - \mathsf{V}'\|^2 =$$

$$= \mathsf{M}\|\mathsf{V}\|^2 + \sum_{i=1}^{\mathsf{n}} m_i\|\boldsymbol{\zeta}_i - \mathsf{V}\|^2 = \sum_{i=1}^{\mathsf{n}} m_i\|\boldsymbol{\zeta}_i\|^2.$$

A collision transformation at a site is written as:

$$P'(S') = W(S \to S')P(S),$$

and the change of the probability distribution in this collision is given by:

$$P'(\boldsymbol{\zeta}_1',\ldots,\boldsymbol{\zeta}_{\mathsf{n}}') = \int\cdots\int \prod_{i=1}^{\mathsf{n}} d\boldsymbol{\zeta}_i \prod_{i=1}^{\mathsf{n}} \delta\big(\boldsymbol{\zeta}_i' - \mathsf{V} + \sigma\big[\boldsymbol{\zeta}_i - \mathsf{V}\big]\big)P(\boldsymbol{\zeta}_1,\ldots,\boldsymbol{\zeta}_{\mathsf{n}}).$$

(2.16)

We observe that the Maxwell distribution,

$$P_m = \prod_{i=1}^{n} \left(\frac{m_i}{2\pi T} \right)^{d/2} e^{-E/T}, \tag{2.17}$$

does not change in collisions and, because it does not depend on particle positions, it is also is invariant under streaming transformations. Thus, we conclude that the Maxwell distribution (2.17) is a stationary solution for an ideal monatomic gas. These arguments can be modified to include more general cases.

Under the molecular chaos assumption the formula (2.16) is further simplified. The probability distribution is expressed as a product of one particle probability distributions:

$$P(\zeta_1, \ldots, \zeta_n) = \prod_{i=1}^{n} P_1(\zeta_i),$$

and, after integration, equation (2.16) takes the form:

$$P_1'(\zeta_1') = \int \cdots \int \prod_{i=1}^{n} d\zeta_i \delta(\zeta_1' - V - \sigma[\zeta_1 - V]) \prod_{i=1}^{n} P_1(\zeta_i).$$

We abbreviate the above formula as:

$$P_1(\zeta_1') + \mathcal{C}(P_1)(\zeta_1') = \int \cdots \int \prod_{i=1}^{n} d\zeta_i \delta(\zeta_1' - V + \sigma[\zeta_1 - V]) \prod_{i=1}^{n} P_1(\zeta_i), \tag{2.18}$$

where $\mathcal{C}$ is the collision operator.

We shall prove that a Maxwell distribution is also a stationary solution of the one-particle reduced collision operator. The method that we employ will

also be used in calculations of transport coefficients in the Chapman-Enskog expansion and autocorrelation functions in the Green-Kubo formulae. We consider the following integral:

$$(\mathcal{J}P_{\mathsf{m}}\phi)(\mathbf{w}) = \sum\!\!\!\!\!\!\int_{\sigma\in O(d)} \int d\mathsf{V}\delta\big(\mathbf{w}-\mathsf{V}+\sigma[\mathsf{V}-\mathbf{v}_1]\big)P_{\mathsf{m}}(\mathbf{V})\phi(\mathbf{v}_1,\mathsf{V}) \qquad (2.19)$$

where $\sum\!\!\!\!\!\!\int$ denotes either sum or integral over a set of rotations. Using the following representation of the delta function:

$$\delta(x) = \frac{1}{2\pi}\int dk e^{ikx},$$

and the identity

$$1 = \mathsf{M}^d \int d\mathsf{V}\delta\Big(\sum_{i=1}^{\mathsf{n}} m_i(\mathsf{V}-\mathbf{v}_i)\Big)$$

we arrive at the expression:

$$(\mathcal{J}P_{\mathsf{m}}\varphi)(\mathbf{w}) = \sum\!\!\!\!\!\!\int_{\sigma\in O(d)} \int d\mathsf{V}d\mathbf{v}_1\delta\big(\mathbf{w}-\mathsf{V}+\sigma[\mathsf{V}-\mathbf{v}_1]\big)\times$$
$$\times\frac{\mathsf{M}^d}{(2\pi)^d}\int d\mathbf{k}\prod_{i=2}^{\mathsf{n}} d\mathbf{v}_i e^{i\mathbf{k}\sum_{i=1}^{\mathsf{n}} m_i(\mathsf{V}-\mathbf{v}_i)}P_{\mathsf{m}}(\mathbf{V})\phi(\mathbf{v}_1,\mathsf{V}).$$

Integrations over $\mathbf{v}_i$, $i=(2,\ldots,\mathsf{n})$ and, afterward, over $\mathbf{k}$ yield the following expression:

$$(\mathcal{J}P_{\mathsf{m}}\phi)(\mathbf{w}) = \sum\!\!\!\!\!\!\int_{\sigma\in O(d)} \int d\mathsf{V}d\mathbf{v}_1\delta\big(\mathbf{w}-\mathsf{V}+\sigma[\mathsf{V}-\mathbf{v}_1]\big)\times$$
$$\times\frac{\mathsf{M}^d}{(2\pi)^d}\exp\left(-\frac{\|\mathsf{M}\mathsf{V}-m_1\mathbf{v}_1\|^2}{2T(\mathsf{M}-m_1)}\right)P_{\mathsf{m}}(\mathbf{v}_1)\phi(\mathbf{v}_1,\mathsf{V}). \qquad (2.20)$$

In the following identity we employed an explicit expression for the value $\mathbf{w}$ after transformation:

$$m_1\|\mathbf{v}_1\|^2 + \frac{\|\mathsf{MV} - m_1\mathbf{v}_1\|^2}{(\mathsf{M}-m_1)} = \mathsf{M}\|\mathsf{V}\|^2 + \frac{\mathsf{M}m_1}{\mathsf{M}-m_1}\|\mathsf{V}-\mathbf{v}_1\|^2 =$$
$$= \mathsf{M}\|\mathsf{V}\|^2 + \frac{\mathsf{M}m_1}{\mathsf{M}-m_1}\|\mathsf{V}-\mathbf{w}\|^2 = m_1\|\mathbf{w}\|^2 + \frac{\|\mathsf{MV} - m_1\mathbf{w}\|^2}{(\mathsf{M}-m_1)},$$

and substitution of the above identity in equation (2.20) gives us the following expression:

$$\left(\mathcal{J}P_{\mathsf{m}}\phi\right)(\mathbf{w}) = P_{\mathsf{m}}(\mathbf{w}) \sum\!\!\!\!\!\!\int_{\sigma\in O(d)} d\mathsf{V} \left[\frac{\mathsf{M}^2}{2\pi T(\mathsf{M}-m_1)}\right]^{d/2} \times$$
$$\times \exp\left(-\frac{\|\mathsf{MV} - m_1\mathbf{w}\|^2}{2T(\mathsf{M}-m_1)}\right) \phi\big(\mathsf{V} + \sigma^{-1}[\mathbf{w}-\mathsf{V}], \mathsf{V}\big). \quad (2.21)$$

In the particular case, when $\phi = 1$, we deduce that the Maxwell distribution is a stationary solution of the collision operator:

$$\left(\mathcal{J}P_{\mathsf{m}}\phi\right)(\mathbf{w}) = P_{\mathsf{m}}(\mathbf{w}).$$

2.5 *Boltzmann equation*

The evolution of the probability distribution of the system under consecutive streaming and collision transformations is governed by the Markov equation with the transition probabilities given by the composition of the corresponding streaming and collision operators. The Boltzmann equation is the evolution equation of the 1-particle probability distribution. From the expressions

for the 1-particle streaming operator, equation (2.7), and the 1-particle collision operator, equation (2.18), we deduce the Boltzmann equation for the lattice gas model:

$$\left[\int_0^1 e^{\tau\mathcal{X}} d\tau\right] \mathcal{X} P_1(1, \mathbf{v}, t) = \mathcal{C}(P_1), \tag{2.22}$$

with the notation of Sec. 2.3.

2.6 Boltzmann H-theorem

In this section we provide a partial result on the convergence of the reduced probability distribution to its stationary form. We consider a specific form of the collision operator as described in the previous section. This collision operator transforms the velocities of incoming particles uniformly. Evolution of the probability distribution on $\mathbb{S}$ is expressed as:

$$P'(\mathbf{W}) = \int d\mathbf{V} \mathcal{T}(\mathbf{V} \to \mathbf{W}) P(\mathbf{V}). \tag{2.23}$$

In order to simplify the proof we introduce some notation.

We shall employ the following result: If $\mathcal{F} : \mathbb{R} \to \mathbb{R}$ is a convex function, $\mathcal{A} : \Omega \to \mathbb{R}$ is some function on Ω and $\mathcal{Z} : \Omega \to \mathbb{R}$ with the restriction on $\mathcal{A}$,

$$\int_\Omega d\omega \mathcal{A}(\omega) = 1 \text{ and } \mathcal{A} \geqslant 0, \tag{2.24}$$

the following inequality holds:

$$\int_\Omega d\omega \mathcal{A}(\omega) \mathcal{F}(\mathcal{Z}(\omega)) \geqslant \mathcal{F}\left(\int_\Omega d\omega \mathcal{A}(\omega) \mathcal{Z}(\omega)\right). \tag{2.25}$$

The above statement says that for a convex function the average of the function is greater than value of the function at the average position.

For each n-particle collision we define the entropy functional H_n by the following formula

$$\mathrm{H}_n(P(\mathbf{V})) = \int d^n\mathbf{V} P(\mathbf{V}) \log(P(\mathbf{V})). \tag{2.26}$$

We prove that for collisions that satisfy semi-detailed balance the total negative entropy H_1 of incoming uncorrelated particles decreases after collision.

The joint probability distribution of uncorrelated colliding particles is given by the expression:

$$P(\mathbf{V}) = \prod_{i=1}^{n} P_i(\mathbf{v}_i) \ . \tag{2.27}$$

By the use of definition (2.26) we arrive at the following relation:

$$\begin{aligned} \mathrm{H}_n(P(\mathbf{V})) &= \int d^n\mathbf{V} P(\mathbf{V}) \log(P(\mathbf{V})) = \\ &= \sum_{j=1}^{n} \int d^n\mathbf{V} \prod_{i=1}^{n} P(\mathbf{v}_i) \log(P_j(\mathbf{v}_j)) = \sum_{j=1}^{n} H_1(P_j(\mathbf{v}_j)) \ . \end{aligned} \tag{2.28}$$

To obtain results on behavour of H_n we need a semi-detailed balance condition:

$$\int d\mathbf{V} \mathcal{T}(\mathbf{V} \to \mathbf{W}) = 1 \ . \tag{2.29}$$

We note that if we replace integration over $d\mathbf{V}$ with integration over $d\mathbf{W}$ the above relation becomes trivial and easily follows from (2.23) and the requirement that the probability density is normalized.

We multiply right-hand side of equation (2.26) with unity and change the order of integration:

$$\mathrm{H}_n(P(\mathbf{V})) = \int d^n\mathbf{V} P(\mathbf{V}) \log(P(\mathbf{V})) \int d^n\mathbf{W} \mathcal{T}(\mathbf{V} \to \mathbf{W}) = \\ = \int d^n\mathbf{W} \int d^n\mathbf{V} \mathcal{T}(\mathbf{V} \to \mathbf{W}) P(\mathbf{V}) \log(P(\mathbf{V})). \quad (2.30)$$

The second integration, due to the semi-detailed balance conditions, satisfies requirement of inequality (2.25) and thus the following relation holds:

$$\mathrm{H}_n(P) \geqslant \int d^n\mathbf{W} \int d\mathbf{V}' \mathcal{T}(\mathbf{V}' \to \mathbf{W}) P(\mathbf{V}') \times \\ \times \log\left(\int d\mathbf{V}'' \mathcal{T}(\mathbf{V}'' \to \mathbf{W}) P(\mathbf{V}'')\right) = \mathrm{H}_n(P'). \quad (2.31)$$

Finally, we show that the 1-entropy of the post-collision particles is smaller than their joint n-entropy. We write postcollision reduced 1-particle probability density as

$$P'_j(\mathbf{v}_j) = \int d\mathbf{v}_1 \cdots \widehat{d\mathbf{v}_j} \cdots d\mathbf{v}_n P'(\mathbf{V}). \quad (2.32)$$

where a hat over a symbol indicates the variable omitted in integration. The integral of P_j over velocities is unity. Using this notation the difference between entropies is written as:

$$\mathrm{H}_n(P'(\mathbf{V})) - \sum_{j=1}^{n} H_1(P'_j(\mathbf{v}_j)) = \int d^n\mathbf{V} P'(\mathbf{V}) \log\left(\frac{P'(\mathbf{V})}{\prod_j P'_j(\mathbf{v}_j)}\right) = \\ = \int d^n\mathbf{V} \prod_j P'_j(\mathbf{v}_j) \frac{P'(\mathbf{V})}{\prod_j P'_j(\mathbf{v}_j)} \log\left(\frac{P'(\mathbf{V})}{\prod_j P'_j(\mathbf{v}_j)}\right) \geqslant \log(1). \quad (2.33)$$

In the above equation we used inequality (2.25) with $\mathcal{F} = x \log x$, $\mathcal{A} = \prod_j P'_j(\mathbf{v}_j)$ and $\mathcal{Z} = \dfrac{P'(\mathbf{V})}{\prod_j P'_j(\mathbf{v}_j)}$.

Combining equations (2.28), (2.31) and (2.33) we arrive at the following inequality that relates pre- and post-collision entropies:

$$\sum_{j=1}^{n} H_1(P_j(\mathbf{v}_j)) \geqslant \sum_{j=1}^{n} H_1(P'_j(\mathbf{v}_j)).$$

To furnish the proof of the H-theorem we show the well-known fact that a Maxwelliam distribution gives a global minimum of the H-functional with fixed velocity and energy of the system.

We use the relation:

$$\int P(\mathbf{V}) \log(P_{\mathsf{m}}(\mathbf{V}))d\mathbf{V} = \int P_{\mathsf{m}}(\mathbf{V}) \log(P_{\mathsf{m}}(\mathbf{V}))d\mathbf{V}. \qquad (2.34)$$

This equation follows from equivalence of energy and momentum expectation values of P and P_{m} and the identity $\log(P_{\mathsf{m}}) = \text{const} - \frac{m(\mathbf{v}-\langle\mathbf{v}\rangle)^2}{2T}$.

From equation (2.34) we derive:

$$H(P) - H(P_{\mathsf{m}}) = \int P(\mathbf{V}) \log\Big(\frac{P(\mathbf{V})}{P_{\mathsf{m}}(\mathbf{V})}\Big)d\mathbf{V} = \\ = \int P_{\mathsf{m}}(\mathbf{V}) \frac{P(\mathbf{V})}{P_{\mathsf{m}}(\mathbf{V})} \log\Big(\frac{P(\mathbf{V})}{P_{\mathsf{m}}(\mathbf{V})}\Big)d\mathbf{V},$$

with right-hand side of the form (2.25). Applying inequality (2.25) we conclude that

$$H(P) \geqslant H(P_{\mathsf{m}}) \text{ for any } P.$$

We have shown that under the molecular chaos assumption the Boltzmann H-functional of the system decreases on each iteration. The Maxwellian distribution is a stationary solution of the collision operator and, simultaneously, is the global minimum of the H-functional. Thus we conclude that at equilibrium particle velocities are distributed according to the Maxwell law.[2]

[2] We remark while the proof follows standard procedures it is not complete and requires additional results on rate of convergence.

3. HYDRODYNAMIC EQUATIONS AND TRANSPORT COEFFICIENTS

3.1 Chapman-Enskog asymptotic expansion

We derive hydrodynamical equations by using an expansion of the reduced probability distribution in slowly varying density fields. This Chapman-Enskog procedure[17] is based on the assumption that any relevant functional can be expanded into a series of partial derivatives of the conserved fields. After scaling $\mathbf{x} \to \epsilon\mathbf{x}$ and $t \to \epsilon t$ the expansion is ordered in powers of ϵ.

It is further assumed that the reduced probability distribution function is defined by the instantaneous spatial distribution of local collision invariants ρ^α.

$$f(\mathbf{x}, \mathbf{v}, t) = f(\mathbf{v}, \boldsymbol{\rho}(\mathbf{x})) = \sum_{n \geqslant 0} \epsilon^n f_n(\mathbf{v}, \boldsymbol{\rho}(\mathbf{x})). \tag{3.1}$$

The density of a local collision invariant is given by the average value

$$\boldsymbol{\rho}(\mathbf{x}) = \langle \boldsymbol{\iota} f(\mathbf{x}, \mathbf{v}, t) \rangle \,, \tag{3.2}$$

and to ensure uniqueness an additional requirement is imposed

$$\langle \iota^{\alpha} f_n(\mathbf{x}, \mathbf{v}, t) \rangle = 0 \text{ for all } n > 0 \text{ and } \alpha, \tag{3.3}$$

where ι is the set of the density, momentum and energy dynamical variables given by equation (2.13a-c).

Time evolution of a functional of conserved quantities is governed by an operator given as an expansion in the small parameter ϵ:

$$\frac{\partial}{\partial t} = \sum_{n \geqslant 0} \epsilon^n \mathcal{D}_n. \tag{3.4}$$

The expansion of the collision operator in a series of ϵ is written formally as:

$$\mathcal{C}(f) = \sum_{n \geqslant 0} \epsilon^n \mathcal{C}_n(\mathbf{f}). \tag{3.5}$$

To make the average of $\langle \mathcal{C}(f) \rangle$ vanish we should set the average of each term of the series to zero $\langle \mathcal{C}_n(\mathbf{f}) \rangle = 0$.

The operator $\mathcal{X}$ takes the form:

$$\mathcal{X} = \epsilon \frac{\partial}{\partial t} - \sum_{n=1}^{\infty} \epsilon^n \frac{\boldsymbol{\kappa}_n(\mathbf{v})}{n!} \boldsymbol{\nabla}^n. \tag{3.6}$$

By expanding the evolution equation (2.22) in powers of ϵ we arrive at the following set of equations:

$$\mathcal{C}_0(\mathbf{f}) = \mathcal{C}(f_0) = 0, \tag{3.7a}$$

$$\mathcal{C}_1(\mathbf{f}) = [\mathcal{D}_0 - \boldsymbol{\nabla} \cdot \boldsymbol{\kappa}_1(\mathbf{v})] f_0, \tag{3.7b}$$

$$\begin{aligned} \mathcal{C}_2(\mathbf{f}) = {} & \mathcal{D}_1 f_0 - [\mathcal{D}_0 + \boldsymbol{\nabla} \cdot \boldsymbol{\kappa}_1(\mathbf{v})] f_1 + \\ & + \frac{1}{2} [\mathcal{D}_0 - \frac{1}{2} \boldsymbol{\nabla} \cdot \boldsymbol{\kappa}_1(\mathbf{v})]^2 f_0 - \boldsymbol{\nabla}^2 : \boldsymbol{\kappa}_2(\mathbf{v}) f_0. \end{aligned} \tag{3.7c}$$

The solution of equation (3.7a) yields a local Maxwellian distribution:

$$f_0 = \sqrt{\frac{m}{2\pi T}}^{d} e^{-\frac{m\|\mathbf{v}-\mathbf{u}\|^2}{2T}} \rho. \tag{3.8}$$

Average of local collision invariants over $\mathbf{v}$ commutes with the operator $\mathcal{D}_i$ so that integration of equation (3.7b) yields

$$\mathcal{D}_0 \rho^\alpha = \boldsymbol{\nabla} \cdot \langle i^\alpha \boldsymbol{\kappa}_1(\mathbf{v}) f_0 \rangle \tag{3.9}$$

The average of equation (3.7c) gives the second order correction to the Euler equations:

$$\mathcal{D}_1 \rho^\alpha = \frac{1}{2} \boldsymbol{\nabla}^2 : \langle i^\alpha \boldsymbol{\kappa}_2(\mathbf{v}) f_0 \rangle - \left\langle i^\alpha [\mathcal{D}_0 - \boldsymbol{\nabla} \cdot \boldsymbol{\kappa}_1(\mathbf{v})](f_1 + \frac{1}{2}\mathcal{C}_1(\mathbf{f})) \right\rangle,$$

and after transformations

$$\mathcal{D}_1 \rho^\alpha = \frac{1}{2} \boldsymbol{\nabla}^2 : \langle i^\alpha \boldsymbol{\kappa}_2(\mathbf{v}) f_0 \rangle + \boldsymbol{\nabla} \cdot \left\langle i^\alpha \boldsymbol{\kappa}_1(\mathbf{v})(f_1 + \frac{1}{2}\mathcal{C}_1(\mathbf{f})) \right\rangle, \tag{3.10}$$

where we used the conditions on $\langle i^\alpha f_1 \rangle$ and $\langle i^\alpha \mathcal{C}_1(\mathbf{f}) \rangle$.

3.2 Navier-Stokes equation

In this section we apply general formulae (3.7a-c) to some collision models. Regardless of the collision model, the equation for the zeroth expansion term has the same form and constitutes the Euler equations of compressible flow. Evaluation of the averages in equation (3.9) yields the following results for

the evolution of the conserved quantities:

$$\frac{\partial}{\partial t}\rho + \nabla_i \rho u_i = 0,$$
$$\frac{\partial}{\partial t}\rho u_j + \nabla_i \rho u_i u_j + \nabla_j \rho T^* = 0,$$
$$\frac{\partial}{\partial t}\left[\frac{1}{2}\rho\|\mathbf{u}\|^2 + \frac{3}{2}\rho T^*\right] + \nabla_i \rho u_i \left[\frac{1}{2}\rho\|\mathbf{u}\|^2 + \frac{5}{2}\rho T^*\right] = 0,$$

where $T^* = T/m$. Algebraic manipulations transform the above system into a set of evolution equations for $\rho, \mathbf{v}$ and T^*:

$$\frac{\partial}{\partial t}\rho + \nabla_i \rho u_i = 0, \tag{3.11a}$$
$$\frac{\partial}{\partial t}u_j + u_i \nabla_i u_j + \frac{1}{\rho}\nabla_j \rho T^* = 0, \tag{3.11b}$$
$$\frac{\partial}{\partial t}T^* + u_i \nabla_i T^* + \frac{2}{3}T \nabla_i u_i = 0. \tag{3.11c}$$

Performing a Laplace - Fourier transform of the linearized version of system (3.11a-c), we arrive at the following system of equations:

$$\begin{bmatrix} z & \mathbf{k}^T & 0 \\ \frac{T^*}{\rho}\mathbf{k} & z & \mathbf{k} \\ 0 & \frac{2}{3}\mathbf{k}^T & z \end{bmatrix} \begin{vmatrix} \rho_k \\ \mathbf{u}_k \\ T_k^* \end{vmatrix} = 0. \tag{3.12}$$

The above system has eigenvalues $z_0 = 0$ and $z_\pm = \pm|\mathbf{k}|\sqrt{\frac{5}{3}T^*}$. Thus there are no dissipative processes in a system governed by (3.11a-c), which can also be seen from the fact that $T^*\rho^{-2/3}$ is conserved along streamlines. The velocity of sound is given by the expression for an ideal monatomic gas:

$$c = \sqrt{\frac{5}{3}T^*}.$$

With the use of equations (3.11a-c) we rewrite equation (3.7b) in the following form:

$$\mathcal{C}_1(\mathbf{f}) = f_0\Big(\frac{\partial \log(f_0)}{\partial \rho}\big[\nabla_i v_i \rho - \nabla_i u_i \rho\big] + \\ + \frac{\partial \log(f_0)}{\partial u_i}\big[\nabla_j v_j u_i - u_j \nabla_j u_i - \frac{1}{\rho}\nabla_i \rho T^*\big] + \\ + \frac{\partial \log(f_0)}{\partial T^*}\big[\nabla_i v_i T^* - u_i \nabla_i T^* - \frac{2}{3} T^* \nabla_i u_i\big]\Big).$$

We substitute the explicit form of f_0 given by equation (3.8) and, after algebraic transformation, arrive at the following equation:

$$\mathcal{C}_1(\mathbf{f}) = f_0\Big(\Big[\frac{\|\mathbf{c}\|^2}{2} - \frac{5}{2}\Big] c_i \nabla_i \log T^* + \frac{1}{T^*}\Big[c_i c_j - \frac{1}{3}\|\mathbf{c}\|^2 \delta_{ij}\Big]\nabla_j u_i\Big), \quad (3.13)$$

where $\mathbf{c} = \mathbf{v} - \mathbf{u}$.

We define the function h_1 by the relation $h_1 f_0 = f_1$. The collision operator $\mathcal{C}_1$ has the following form:

$$\mathcal{C}_1(\mathbf{f})(\mathbf{w}) + f_1(\mathbf{w}) = \sum_{n=1}^{\infty} \frac{\rho^n}{(n-1)!} e^{-\rho} \times \\ \times \sum\!\!\!\!\!\!\int_{\sigma \in O(d)} d\mathbf{V} \delta(\mathbf{w} - \mathbf{V} + \sigma(\mathbf{V} - \mathbf{v}_1)) P_{\mathsf{m}}(\mathbf{V}) \sum_{i=1}^{n} h_1(\mathbf{v}_i), \quad (3.14)$$

using the notation of Sec. 2.13.

Equations (3.14) and (3.13) constitute a linear integral equation for the function h_1, which can be split into two equations, one that involves terms $\boldsymbol{\nabla} \log T^*$ and the other that depends on gradients of velocity fields.

With use of the approach developed in Sec. 2.13 we shall show that

$$h_1 = \Big[c_i c_j - \frac{1}{3}\|\mathbf{c}\|^2 \delta_{ij}\Big]$$

is an eigenfunction of the collision operator and its corresponding eigenvalue defines the value of the viscosity coefficient. Namely, with the use of identity:

$$1 = n^d \int d\mathsf{V} \exp\bigl(i\mathbf{k} \cdot \sum_{i=1}^{\mathsf{n}} (\mathsf{V} - \mathbf{v}_i)\bigr),$$

and subsequent integration over $\mathbf{v}_i$, $i = (2, \ldots, \mathsf{n})$, equation (3.14) can be reduced to the sum of the following integrals:

$$I = \sum\!\!\!\!\!\!\int_{\sigma \in O(d)} \int d\mathsf{V} d\mathbf{c}_1 \delta(\mathbf{w} - \mathsf{V} + \sigma(\mathsf{V} - \mathbf{c}_1)) \frac{n^d}{(2\pi)^d} \times$$
$$\times \int d\mathbf{k} e^{-T^*(n-1)\|\mathbf{k}\|^2/2 + i\mathbf{k}\cdot(n\mathsf{V} - \mathbf{c}_1)} \left[(n-1)k_x k_y + \frac{1}{T^*} c_{1x} c_{1y}\right]. \quad (3.15)$$

Evaluation of the above integral for the collision models discussed in Sec. 2.2.3 proves that $c_x c_y$ is an eigenfunction and gives us the eigenvalues:

$$\gamma = \frac{1 - \rho - e^{-\rho}}{\rho} \quad \text{and} \quad \gamma = 2\frac{1 - \rho - e^{-\rho}}{\rho},$$

for uniformly scattered collisions and collisions with $\pi/2$ rotations, respectively.

Evaluation of the averages in equation (3.10) yields the following expressions for the second order terms in the Chapman-Enskog expansion:

$$\mathcal{D}_1 \rho = D\Delta\rho, \quad (3.16)$$

$$\mathcal{D}_1 \rho u_i = D\Delta\rho u_i - \nabla_j \pi_{ij}, \quad (3.17)$$

$$\mathcal{D}_1 \left[\frac{1}{2}\rho\|\mathbf{u}\|^2 + \frac{3}{2}\rho T^*\right] = D\Delta\left[\frac{1}{2}\rho\|\mathbf{u}\|^2 + \frac{3}{2}\rho T^*\right] - \nabla_i u_j \pi_{ij} + \frac{3}{2}\nabla_i \lambda \nabla_i T^*, \quad (3.18)$$

where λ is thermal conductivity coefficient and the irreversible contribution to the pressure tensor is given by the following expression:

$$\pi_{ij} = \rho T^* \left[\frac{1}{2} + \frac{1}{\gamma}\right] \left(\nabla_i u_j + \nabla_j u_i - \frac{2}{3}\delta_{ij}\nabla_k u_k\right). \tag{3.19}$$

We observe that in the above equation the density continuity equation has an additional flux term $D\Delta\rho$ which can be conveniently rewritten as $\nabla_i \rho D \nabla_i \log\rho$. Thus, in the new set of variables $\mathbf{w} = \mathbf{u} - D\boldsymbol{\nabla}\log\rho$, the continuity equation assumes the familiar form:

$$\frac{\partial}{\partial t}\rho + \nabla_i w_i \rho = 0.$$

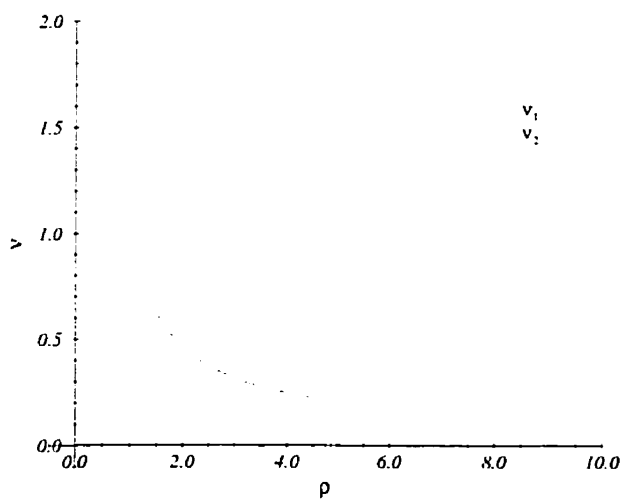

Kinematic viscosity for different collision models at $T^* = 1$. Fig. 3.1

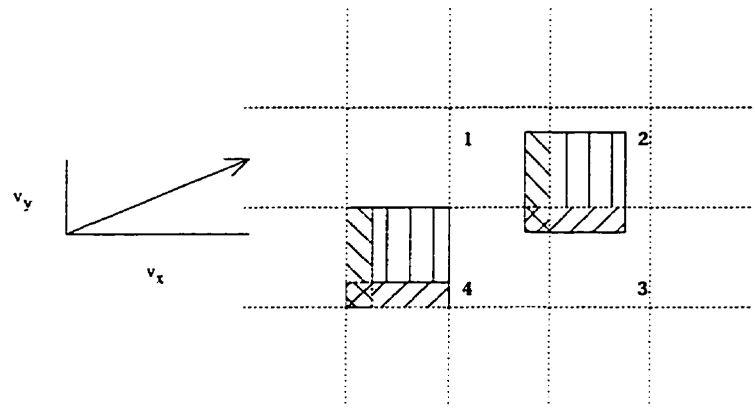

Fig. 3.2 Pictorial representation of the streaming transformation in the stochastic model.

The form of the continuity equation suggests that we look for the hydrodynamic equations in the new set of variables $(\rho, \mathbf{w}, T^*)$. After algebraic transformations we arrive at the following set of equations:

$$\frac{\partial}{\partial t}\rho + \nabla_i w_i \rho = 0, \tag{3.20a}$$

$$\frac{\partial}{\partial t} w_i + w_j \nabla_j w_i + \frac{1}{\rho}\nabla_i \rho T^* = -\frac{1}{\rho}\nabla_j \pi'_{ij}, \tag{3.20b}$$

$$\frac{\partial}{\partial t} T^* + w_i \nabla_i T^* + \frac{2}{3} T^* \nabla_i w_i = -\frac{2}{3\rho}\pi'_{ij}\nabla_i w_j \pi_{ij} - \frac{2D}{3}\nabla_i w_j \nabla_j w_i + \\ + \frac{1}{\rho}\nabla_i (D\rho + \lambda)\nabla_i T^* - \frac{2}{3} T^* \Delta \log \rho. \tag{3.20c}$$

We observe that in the new variables evolutions of velocity, temperature and density fields are governed by the Navier-Stokes equation with the following pressure tensor:

$$\pi'_{ij} = \pi_{ij} - \rho D(\nabla_i w_j + \nabla_j w_i)$$

The above expression does have a Newton pressure tensor form with values of shear and bulk viscosity coefficients $\eta' = \eta + D\rho$ and $\eta'_B = \eta_B + 2D\rho/3$, respectively. The pressure tensor is spherically symmetric and, for the collision models discussed above, has vanishing bulk viscosity coefficient $\eta_B = 0$.

In Fig. 3.1 we plot the values of shear viscosity coefficients for the models. Equation (3.19) gives us the following values:

$$\eta'_1 = \rho D + \rho T^* \frac{1 + \rho - e^{-\rho}}{2\big(e^{-\rho} - (1-\rho)\big)},$$

and

$$\eta'_2 = \rho D + \rho T^* \frac{1 - e^{-\rho}}{2\big(e^{-\rho} - (1-\rho)\big)}.$$

The modified bulk viscosity coefficient has the same value in both models $\eta'_B = 2D\rho/3$.

At this point we give a physical explanation for why the change of variables $\mathbf{w} = \mathbf{u} - D\nabla \log \rho$ leads to the Navier-Stokes equations. In Fig. 3.2 we compare deterministic streaming of particles with its stochastic counterpart. The deterministic streaming transfers particles from the shaded domain to the similarly shaded translated domain. If in the initial domain the particle density was not uniform, the probabilities of transfer into domain pairs (1,4) and (3,4) are $(1-\{v_x\})\rho + (1-\{v_x\})\{v_x\}\nabla_x\rho/2$ and $\{v_x\}\rho - (1-\{v_x\})\{v_x\}\nabla_x\rho/2$, respectively.[1] In the stochastic models we consider systems which consist of cells with uniform particle density and the correction term $\kappa_2(\mathbf{v})$ does not

[1] The cell edge length is set to unity.

enter the equations. The change of variables $\mathbf{w} = \mathbf{u} - D\nabla \log \rho$ accounts for the correction term and reduces system to the Navier-Stokes equations.

4. GREEN-KUBO FORMULAE AND COMPUTATION OF TRANSPORT COEFFICIENTS

In this section we develop a projection operator formalism and derive Green-Kubo formulae for discrete systems. We obtain important results as a consequence of the description of the system in terms of linear response, such as Onsager relations for discrete systems. The approach developed here will be used to derive expressions for transport coefficient for various relaxation processes.

4.1 Green-Kubo formulae

The approach we chose follows the lines of the well-known reduction of the classical evolution of a Hamiltonian system to a generalized Langevin equation.[18] However, the intrinsic stochasticity of the model and discreteness of the system introduces unique features in the derivation of Green-Kubo formulae that require special treatment.

4.1.1 Projected dynamics

We define a projection operator as follows:

$$(\mathcal{P}H)(\Gamma) = H_{\mathcal{P}}(\Gamma) = \mathbf{a}^{\dagger}(\Gamma)P_0(\Gamma)\left\langle \mathbf{a}\mathbf{a}^{\dagger}\right\rangle^{-1}\int d\Gamma' \mathbf{a}(\Gamma')H(\Gamma'), \tag{4.1}$$

where $\mathbf{a}$ is a set of dynamical variables. The operator $\mathcal{P}$ is indeed a projection operator. By direct application of the operator twice we verify the identity $\mathcal{P}\mathcal{P} = \mathcal{P}$. We define a complimentary operator $\mathcal{Q}$ by the following relation:

$$\mathcal{Q} + \mathcal{P} = \hat{1}. \tag{4.2}$$

By acting on the identity (4.2) with the operator $\mathcal{P}$ from the left and from the right we prove orthogonality of the operators $\mathcal{P}$ and $\mathcal{Q}$;

$$\mathcal{P}\mathcal{Q} = \mathcal{Q}\mathcal{P} = \hat{0}. \tag{4.3}$$

By acting on the identity (4.2) with the operator $\mathcal{Q}$ and using the orthogonality condition (4.3) we find that $\mathcal{Q}$ is a projection operator; $\mathcal{Q}\mathcal{Q} = \mathcal{Q}$.

We consider the evolution of the probability distribution $\mathrm{P}(\Gamma, t)$ governed by the transition operator $\mathcal{W}$;

$$\mathrm{P}(\Gamma, t+1) = \int d\Gamma' \mathcal{W}(\Gamma' \to \Gamma)\mathrm{P}(\Gamma', t), \tag{4.4}$$

where the integral sign implies summation over discrete variables. In what follows we shall often drop the argument Γ. We separate the above equation into a system of two equations:

$$\mathrm{P}_{\mathcal{P}}(t+1) = \mathcal{P}\mathcal{W}\big(\mathrm{P}_{\mathcal{P}}(t) + \mathrm{P}_{\mathcal{Q}}(t)\big),$$

$$\mathrm{P}_{\mathcal{Q}}(t+1) = \mathcal{Q}\mathcal{W}\big(\mathrm{P}_{\mathcal{P}}(t) + \mathrm{P}_{\mathcal{Q}}(t)\big).$$

Using relation (4.3) we transform the above system into

$$\mathrm{P}_{\mathcal{P}}(t+1) = \mathcal{P}\mathcal{W}\mathrm{P}_{\mathcal{P}}(t) + \mathcal{P}(\mathcal{W}-\hat{1})\mathrm{P}_{\mathcal{Q}}(t), \tag{4.5}$$

$$\mathrm{P}_{\mathcal{Q}}(t+1) = \mathcal{Q}(\mathcal{W}-\hat{1})\mathrm{P}_{\mathcal{P}}(t) + \mathcal{Q}\mathcal{W}\mathrm{P}_{\mathcal{Q}}(t). \tag{4.6}$$

A recursive application of equation (4.6) yields the following equation:

$$\mathrm{P}_{\mathcal{Q}}(t) = [\mathcal{Q}\mathcal{W}]^{t}\mathrm{P}_{\mathcal{Q}}(0) + \sum_{\tau=1}^{t}[\mathcal{Q}\mathcal{W}]^{\tau-1}\mathcal{Q}(\mathcal{W}-\hat{1})\mathrm{P}_{\mathcal{P}}(t-\tau), \tag{4.7}$$

which, after substitution into equation (4.5), yields

$$\mathrm{P}_{\mathcal{P}}(t+1) = \mathcal{P}\mathcal{W}\mathrm{P}_{\mathcal{P}}(t) + \mathcal{P}(\mathcal{W}-\hat{1})\sum_{\tau=1}^{t}[\mathcal{Q}\mathcal{W}]^{\tau-1}\mathcal{Q}(\mathcal{W}-\hat{1})\mathrm{P}_{\mathcal{P}}(t-\tau). \tag{4.8}$$

We eliminated the first term of right-hand side of the relation (4.7) by the use of a specially prepared ensemble of initial conditions, where deviations in only the dynamical variables occur. For slowly decaying dynamical variables, which are our main concern, $\mathrm{P}_{\mathcal{P}}(t-\tau)$ can be replaced by $\mathrm{P}_{\mathcal{P}}(t)$.

For convenience of the subsequent discussion we introduce an operator $\mathcal{S}(\Gamma, t)$ which relates to the state Γ at the initial time the set of states after t steps of evolution, weighted with the probability of transition to the corresponding state. Using this notation we may express equilibrium averages in the following form:

$$\int d\Gamma a(\Gamma)\mathcal{W}(\Gamma' \to \Gamma)b(\Gamma')P_0(\Gamma') = \langle a(\mathcal{S}(\Gamma,1))b(\Gamma)\rangle\,,$$

where summation over states is implied.

4.1.2 k-dependence of the operator $\mathcal{P}(\mathcal{W} - \hat{1})$

Our main interest lies in spatial dynamical variables for small $\mathbf{k}$.

We consider a particular case of projection operators defined by locally conserved quantities. In $\mathbf{k}$-space such quantities are expressed as

$$a_{\mathbf{k}}(\Gamma(t)) = \sum_n \iota_n(t) e^{i\mathbf{k}\cdot\mathbf{r}_n(t)},$$

and, for the dynamics given by a composition of streaming and collision in that order, the following identity holds:

$$\sum_n \iota_n(t) e^{i\mathbf{k}\cdot\mathbf{r}_n(t)} = \sum_n \iota_n(t-1) e^{i\mathbf{k}\cdot\mathbf{r}_n(t)}. \tag{4.9}$$

Equation (4.9) follows from the conservation of the quantities ι under collisions at time $t+1$.

Using identity (4.9) and expanding $\mathbf{a}$ in powers of $\mathbf{k}$, we write the $\mathcal{P}$-projection of $[\mathcal{W} - \hat{1}]b$, where b is an arbitrary function as:

$$\begin{aligned}
&(\mathcal{P}[\mathcal{W} - \hat{1}]b)(\Gamma) = \\
&\quad = \mathbf{a}^\dagger(\Gamma) P_0(\Gamma) \left\langle \mathbf{a}\mathbf{a}^\dagger \right\rangle^{-1} \int d\Gamma' \left[\mathbf{a}(\mathcal{S}(\Gamma', 1)) - \mathbf{a}(\Gamma')\right] b(\Gamma') = \\
&\quad\quad = \mathbf{a}^\dagger(\Gamma) P_0(\Gamma) \left\langle \mathbf{a}\mathbf{a}^\dagger \right\rangle^{-1} \int d\Gamma' \Big[e^{i\mathbf{k}\cdot\mathbf{r}'_n(t)} b(\Gamma') \times \\
&\quad\quad\quad \times \sum_n \left(i\mathbf{k}\cdot\left[\mathbf{r}'_n(1) - \mathbf{r}'_n(0)\right]\iota'_n(0) + o(\mathbf{k})\right) \Big].
\end{aligned} \tag{4.10}$$

Along the same lines we may prove that $[\mathcal{W} - \hat{1}]\mathcal{P} = O(\mathbf{k})$.

With the use of the above identity (4.10) we recast the expression for the memory kernel as

$$\mathcal{K}(\tau) = \mathcal{P}(\mathcal{W} - \hat{1})\left[\mathcal{Q}\mathcal{W}\right]^{\tau}\mathcal{Q}(\mathcal{W} - \hat{1})\mathcal{P}. \tag{4.11}$$

Our aim is to prove

$$\left[\mathcal{Q}\mathcal{W}\right]^{n}\mathcal{Q} = \mathcal{Q}\mathcal{W}^{n}\mathcal{Q} + o(\mathbf{k}). \tag{4.12}$$

For $n = 0$ the relation (4.12) holds. Let us assume that it holds for $n = N$ and prove the relation for $n = N + 1$. We write $\left[\mathcal{Q}\mathcal{W}\right]^{N+1}\mathcal{Q} = \left[\mathcal{Q}\mathcal{W}\right]^{N}\mathcal{Q}\mathcal{W}\mathcal{Q}$. Then

$$\begin{aligned}\left[\mathcal{Q}\mathcal{W}\right]^{N+1}\mathcal{Q} = \left[\mathcal{Q}\mathcal{W}\right]^{N}\mathcal{Q}\mathcal{W}\mathcal{Q} = \mathcal{Q}\mathcal{W}^{N}\mathcal{Q}\mathcal{W}\mathcal{Q} + o(\mathbf{k}) = \\ = \mathcal{Q}\mathcal{W}^{N}\left[\mathcal{Q} + (\mathcal{W} - \hat{1}) + o(\mathbf{k})\right]\mathcal{Q} + o(\mathbf{k}) = \mathcal{Q}\mathcal{W}^{N+1}\mathcal{Q} + o(\mathbf{k}),\end{aligned} \tag{4.13}$$

where we re-expressed $\mathcal{Q}\mathcal{W}$ in the equivalent form

$$\mathcal{Q}\mathcal{W} = \mathcal{Q} + (\mathcal{W} - \hat{1}) - \mathcal{P}(\mathcal{W} - \hat{1}) = \mathcal{Q} + (\mathcal{W} - \hat{1}) + o(\mathbf{k}). \tag{4.14}$$

We proved the assertion of the recursion and, thus, the formula (4.12).

From the relation (4.10), its dual expression, and the formula (4.12) we express the memory kernel equation as:

$$\mathcal{K}(\tau) = \mathcal{P}(\mathcal{W} - \hat{1})\mathcal{Q}\mathcal{W}^{\tau}\mathcal{Q}(\mathcal{W} - \hat{1})\mathcal{P}$$

4.1.3 Symmetry of time-correlation function

Due to their nature, stochastic models do not possess time reversal symmetry. However, for time-correlation functions involving averages over the

equilibrium distribution we may obtain some partial results. We express the time-correlation of dynamical variables a_i and a_j in integral form:

$$\langle a_{\mathbf{k}i}(\mathcal{S}(\Gamma,t))a^*_{\mathbf{k}j}(\Gamma)\rangle = \iint d\Gamma d\Gamma' P(\Gamma,t|\Gamma',0)a_{\mathbf{k}i}(\Gamma)a^*_{\mathbf{k}j}(\Gamma'). \qquad (4.15)$$

For each state Γ we define a pre-collision state $\hat{\Gamma}$, where we use the same ordering of collision and streaming operators as in Sec. 4.1.2. If $\mathbf{a_k}$ is a set of locally conserved dynamical variables the value of the correlation function is invariant with respect to change of Γ to $\hat{\Gamma}$. An analysis of the model shows that transition probabilities of $\Gamma' \to \Gamma$ and $\hat{\Gamma} \to \hat{\Gamma}'$ are equal after we reverse the velocity direction. During evolution the equilibrium distribution also remains constant so that by performing a change of variables in (4.15) we arrive at the following identity:

$$\langle a_{\mathbf{k}i}(\mathcal{S}(\Gamma,t))a^*_{\mathbf{k}j}(\Gamma)\rangle = \langle a^*_{-\mathbf{k}j}(\mathcal{S}(\Gamma,t))a_{-\mathbf{k}i}(\Gamma)\rangle,$$

or in the matrix form:

$$\left\langle \mathbf{a_k}(\mathcal{S}(\Gamma,t))\mathbf{a}^\dagger_{\mathbf{k}}(\Gamma)\right\rangle^\dagger = \left\langle \mathbf{a}_{-\mathbf{k}}(\mathcal{S}(\Gamma,t))\mathbf{a}^\dagger_{-\mathbf{k}}(\Gamma)\right\rangle. \qquad (4.16)$$

Equation (4.16) constitutes the Onsager relations for discrete models. The above derivation relied on the invariance of the dynamical variables with respect to the collision transformation. In general one may obtain similar relations for dynamical variables of the form $\frac{1}{2}(b(\Gamma)+b(\hat{\Gamma}))$.

4.1.4 Evolution of the locally conserved quantities

The average of a set of conserved quantities over the projected probability distribution (4.8) yields evolution equation for these quantities. In a vector forms they read:

$$\bar{\mathbf{a}}(t+1) - \bar{\mathbf{a}}(t) = \left\langle \left(\mathbf{a}(\mathcal{S}(\Gamma,1)) - \mathbf{a}(\Gamma)\right)\mathbf{a}^\dagger(\Gamma)\right\rangle \left\langle \mathbf{a}\mathbf{a}^\dagger\right\rangle^{-1} \bar{\mathbf{a}}(t) + \\ + \sum_{\tau=1}^{t} \left\langle \mathbf{a}\left(\mathcal{W}-\hat{1}\right)\mathcal{Q}\mathcal{W}^{\tau-1}\mathcal{Q}\left(\mathcal{W}-\hat{1}\right)\mathbf{a}^\dagger\right\rangle \left\langle \mathbf{a}\mathbf{a}^\dagger\right\rangle^{-1} \bar{\mathbf{a}}(t-\tau). \quad (4.17)$$

We rewrite the first term on the right-hand side of equation (4.17) as a sum of symmetric and antisymmetric operators as:

$$\left\langle \left(\mathbf{a}(\mathcal{S}(\Gamma,1)) - \mathbf{a}(\Gamma)\right)\mathbf{a}^\dagger(\Gamma)\right\rangle = \frac{1}{2}\left\langle \mathbf{a}(\mathcal{S}(\Gamma,1))\mathbf{a}^\dagger(\Gamma) - \mathbf{a}(\Gamma)\mathbf{a}^\dagger(\mathcal{S}(\Gamma,1))\right\rangle - \\ - \frac{1}{2}\left\langle \left(\mathbf{a}(\mathcal{S}(\Gamma,1)) - \mathbf{a}(\Gamma)\right)\left(\mathbf{a}^\dagger(\mathcal{S}(\Gamma,1)) - \mathbf{a}^\dagger(\Gamma)\right)\right\rangle, \quad (4.18)$$

where we used time-translation invariance of the equilibrium probability distribution

$$\left\langle \mathbf{a}(\mathcal{S}(\Gamma,1))\mathbf{a}^\dagger(\mathcal{S}(\Gamma,1))\right\rangle = \left\langle \mathbf{a}(\Gamma)\mathbf{a}^\dagger(\Gamma)\right\rangle.$$

For the memory kernel acting on $\left\langle \mathbf{a}\mathbf{a}^\dagger\right\rangle^{-1}\bar{\mathbf{a}}$ we write

$$\left\langle \mathbf{a}\left(\mathcal{W}-\hat{1}\right)\mathcal{Q}\mathcal{W}^{t-1}\mathcal{Q}\left(\mathcal{W}-\hat{1}\right)\mathbf{a}^\dagger\right\rangle = \left\langle \mathbf{f}(t)\tilde{\mathbf{f}}(0)\right\rangle, \quad (4.19)$$

where

$$\mathbf{f}(t) = \mathbf{a}(\mathcal{S}(\Gamma,t+1)) - \left\langle \mathbf{a}(\mathcal{S}(\Gamma',1))\mathbf{a}^\dagger(\Gamma')\right\rangle \left\langle \mathbf{a}\mathbf{a}^\dagger\right\rangle^{-1} \mathbf{a}(\mathcal{S}(\Gamma,t)), \quad (4.20)$$

$$\tilde{\mathbf{f}}(0) = \mathbf{a}^\dagger(\Gamma) - \mathbf{a}^\dagger(\mathcal{S}(\Gamma,1)) \left\langle \mathbf{a}\mathbf{a}^\dagger\right\rangle^{-1} \left\langle \mathbf{a}(\mathcal{S}(\Gamma',1))\mathbf{a}^\dagger(\Gamma')\right\rangle.$$

We shall show that the memory kernel can be represented in form of a "force-force" time-correlation function. The sum $\mathbf{f}^\dagger(0) + \bar{\mathbf{f}}(0)$ is of order $\mathbf{k}^2$ as can be seen from the following relation:

$$\begin{aligned}
&\mathbf{a}^\dagger(\mathcal{S}(\Gamma,1)) - \mathbf{a}^\dagger(\Gamma)\left\langle \mathbf{a}\mathbf{a}^\dagger\right\rangle^{-1}\left\langle \mathbf{a}(\Gamma')\mathbf{a}^\dagger(\mathcal{S}(\Gamma',1))\right\rangle + \\
&\qquad + \mathbf{a}^\dagger(\Gamma) - \mathbf{a}^\dagger(\mathcal{S}(\Gamma,1))\left\langle \mathbf{a}\mathbf{a}^\dagger\right\rangle^{-1}\left\langle \mathbf{a}(\mathcal{S}(\Gamma',1))\mathbf{a}^\dagger(\Gamma')\right\rangle = \\
&\quad = \frac{1}{2}\left(\mathbf{a}^\dagger(\Gamma) - \mathbf{a}^\dagger(\mathcal{S}(\Gamma,1))\right)\left\langle \mathbf{a}(\mathcal{S}(\Gamma,1))\mathbf{a}^\dagger(\Gamma) - \mathbf{a}(\Gamma)\mathbf{a}^\dagger(\mathcal{S}(\Gamma,1))\right\rangle + \\
&+ \frac{1}{2}\left(\mathbf{a}^\dagger(\Gamma) + \mathbf{a}^\dagger(\mathcal{S}(\Gamma,1))\right)\left\langle \left[\mathbf{a}(\Gamma') - \mathbf{a}(\mathcal{S}(\Gamma',1))\right]\left[\mathbf{a}^\dagger(\Gamma') - \mathbf{a}^\dagger(\mathcal{S}(\Gamma',1))\right]\right\rangle,
\end{aligned}$$

where we used time-translation invariance of equilibrium averages in the same way as in equation (4.18). If $\mathbf{a}$ are locally conserved variables then both terms on the right-hand side of the above formula are of order $\mathbf{k}$ and, thus, the difference is of order $\mathbf{k}^2$.

We introduce notation $\mathbf{b}(\Gamma) = \mathbf{a}(\Gamma) - \mathbf{a}(\mathcal{S}(\Gamma,1))$. We write the second term of the equation (4.18) as:

$$\frac{1}{2}\left\langle \mathbf{b}(\Gamma)\mathbf{b}^\dagger(\Gamma)\right\rangle = \frac{1}{2}\left\langle \mathbf{b}(\Gamma)\mathcal{Q}\mathbf{b}^\dagger(\Gamma)\right\rangle + \frac{1}{2}\left\langle \mathbf{b}(\Gamma)\mathcal{P}\mathbf{b}^\dagger(\Gamma)\right\rangle. \tag{4.21}$$

First, we notice that $\mathcal{Q}\mathbf{b}^\dagger(\Gamma) = \mathbf{f}^\dagger(0)$ and, thus, the first term has the same form as the summands of the memory kernel: $\left\langle \frac{1}{2}\mathbf{f}\mathbf{f}^\dagger\right\rangle$. The second term in the above equation we expressed as:

$$\begin{aligned}
\left\langle \mathbf{b}(\Gamma)\mathcal{P}\mathbf{b}^\dagger(\Gamma)\right\rangle = &-\left\langle \left(\mathbf{a}(\mathcal{S}(\Gamma,1)) - \mathbf{a}(\Gamma)\right)\mathbf{a}^\dagger(\Gamma)\right\rangle \times \\
&\times \left\langle \mathbf{a}\mathbf{a}^\dagger\right\rangle^{-1}\left\langle \mathbf{a}(\Gamma)\left(\mathbf{a}^\dagger(\mathcal{S}(\Gamma,1)) - \mathbf{a}^\dagger(\Gamma)\right)\right\rangle
\end{aligned}$$

Furthermore, we show that:

$$\left[\frac{1}{2}\left\langle \mathbf{a}(\mathcal{S}(\Gamma,1))\mathbf{a}^{\dagger}(\Gamma)-\mathbf{a}(\Gamma)\mathbf{a}^{\dagger}(\mathcal{S}(\Gamma,1))\right\rangle \left\langle \mathbf{a}\mathbf{a}^{\dagger}\right\rangle^{-1}\right]^{2}=$$

$$=-\left\langle \mathbf{b}(\Gamma)\mathcal{P}\mathbf{b}^{\dagger}(\Gamma)\right\rangle \left\langle \mathbf{a}\mathbf{a}^{\dagger}\right\rangle^{-1}+o(\mathbf{k}^{2}).$$

Indeed,

$$\frac{1}{2}\left\langle \mathbf{a}(\mathcal{S}(\Gamma,1))\mathbf{a}^{\dagger}(\Gamma)-\mathbf{a}(\Gamma)\mathbf{a}^{\dagger}(\mathcal{S}(\Gamma,1))\right\rangle -\left\langle \left(\mathbf{a}(\mathcal{S}(\Gamma,1))-\mathbf{a}^{\dagger}(\Gamma)\right)\mathbf{a}(\Gamma)\right\rangle =$$

$$=\frac{1}{2}\left\langle \left[\mathbf{a}(\Gamma')-\mathbf{a}(\mathcal{S}(\Gamma',1))\right]\left[\mathbf{a}^{\dagger}(\Gamma')-\mathbf{a}^{\dagger}(\mathcal{S}(\Gamma',1))\right]\right\rangle =o(\mathbf{k}),$$

with the similar expression for the second factor.

Now we consider a general question about discrete time dynamics. Suppose that time evolution of the system is given by the following Euler scheme:

$$\bar{a}(t+1)=\bar{a}(t)+\left[\mathcal{A}-\mathcal{B}\right]\bar{a}(t),$$

where $\mathcal{A}$ and $\mathcal{B}$ are of the first and second orders in $\mathbf{k}$. In this case we write the operator identity:

$$\exp\left(\frac{\partial}{\partial t}\right)=\hat{1}+\mathcal{A}-\mathcal{B},$$

or, by expanding the logarithm into a Taylor series up to second order in $\mathbf{k}$:

$$\frac{\partial}{\partial t}=\mathcal{A}-\frac{1}{2}\mathcal{A}^{2}-\mathcal{B}. \tag{4.22}$$

Combining equations (4.22), (4.21), (4.18) and (4.19) we arrive at the following expression for the time evolution of ensemble averages of locally conserved

dynamical variables $\mathbf{a}$:

$$\bar{\mathbf{a}}_t = \frac{1}{2}\left\langle \mathbf{a}(\mathcal{S}(\Gamma,1))\mathbf{a}^\dagger(\Gamma) - \mathbf{a}(\Gamma)\mathbf{a}^\dagger(\mathcal{S}(\Gamma,1))\right\rangle \left\langle \mathbf{a}\mathbf{a}^\dagger\right\rangle^{-1}\bar{\mathbf{a}} - \\ - \left[\frac{1}{2}\left\langle \mathbf{f}(0)\mathbf{f}^\dagger(0)\right\rangle + \sum_{t=1}^{\infty}\left\langle \mathbf{f}(t)\mathbf{f}^\dagger(0)\right\rangle\right]\left\langle \mathbf{a}\mathbf{a}^\dagger\right\rangle^{-1}\bar{\mathbf{a}}. \quad (4.23)$$

We note that the sum of the force-force time-correlation function is represented by a trapezoid approximation of the continuous time integral.

In some cases equation (4.23) admits a further reduction. We may separate a random component due to stochastic nature of the streaming operator from the force-force auto-correlation function. Indeed, the correlations of streaming operator enter equation (4.23) only through term $\left\langle \mathbf{f}(0)\mathbf{f}^\dagger(0)\right\rangle$.

We consider the evolution of a set of conserved dynamical variables $\mathbf{f_k} = \mathbf{g}e^{i\mathbf{k}\cdot\mathbf{l}}$, where $\mathbf{g}$ depends only on the internal state of the particles. In this case the force-force auto-correlator at time zero can be split in two parts:

$$\left\langle \mathbf{f_k}\mathbf{f_k}^\dagger\right\rangle = -D\mathbf{k}\mathbf{k}\left\langle \mathbf{g}\mathbf{g}^\dagger\right\rangle + \left\langle \mathbf{g}\mathbf{v}(\mathbf{g}\mathbf{v})^\dagger\right\rangle \quad (4.24)$$

where D is the same as in equation (2.12).

4.2 Hydrodynamic equations in Green-Kubo formalism

In this section we present a derivation of the hydrodynamic equations. We apply equation (4.23) to a complete set of independent conserved quantities in the system. It is convenient to work with an orthogonal set of dynamical

variables. From the system of equations (2.13a-c) we construct the following set:

$$\mathbf{a_k} = \{\rho_\mathbf{k}, \mu_\mathbf{k}, s_\mathbf{k}\},$$

where we introduce the notation $s_\mathbf{k} = \varepsilon_\mathbf{k} - 3T\rho_k/2$ and we consider particles of unit mass so that $T^* = T$.

The cross-correlation matrix is indeed diagonal and has the following form:

$$\left\langle \mathbf{a_k} \mathbf{a_k^\dagger} \right\rangle = N \begin{pmatrix} 1 & 0 & 0 & 0 & 0 \\ 0 & T & 0 & 0 & 0 \\ 0 & 0 & T & 0 & 0 \\ 0 & 0 & 0 & T & 0 \\ 0 & 0 & 0 & 0 & c_v T^2 \end{pmatrix}, \tag{4.25}$$

where $c_v = 3/2$ in the case of three dimensions and N is the number of particles.

The dissipation free evolution is defined by the following equation:

$$\frac{1}{2}\left\langle \mathbf{a_k}(\mathcal{S}(\Gamma,1))\mathbf{a_k^\dagger}(\Gamma) - \mathbf{a_k}(\Gamma)\mathbf{a_k^\dagger}(\mathcal{S}(\Gamma,1)) \right\rangle =$$

$$= N \begin{pmatrix} 0 & ik_xT & ik_yT & ik_zT & 0 \\ ik_xT & 0 & 0 & 0 & ik_xT^2 \\ ik_yT & 0 & 0 & 0 & ik_yT^2 \\ ik_zT & 0 & 0 & 0 & ik_zT^2 \\ 0 & ik_xT^2 & ik_yT^2 & ik_zT^2 & 0 \end{pmatrix}. \tag{4.26}$$

From equation (4.20) we find the expressions for the forces:

$$f^{\rho}_{\mathbf{k}}(t) = i\mathbf{k}\cdot\sum_i\left[\boldsymbol{\xi}_i(t+1)-\boldsymbol{\xi}_i(t)-\boldsymbol{\zeta}_i\right]+o(\mathbf{k}), \tag{4.27}$$

$$f^{\mu}_{\mathbf{k}}(t) = \sum_i\left(\boldsymbol{\zeta}_i(t)\left[\mathbf{k}\cdot(\boldsymbol{\xi}_i(t+1)-\boldsymbol{\xi}_i(t))\right]-\frac{1}{3}i\mathbf{k}\|\boldsymbol{\zeta}_i(t)\|^2\right)+o(\mathbf{k}), \tag{4.28}$$

$$f^{\varepsilon}_{\mathbf{k}}(t) = i\mathbf{k}\cdot\sum_i\left[\boldsymbol{\xi}_i(t+1)-\boldsymbol{\xi}_i(t)-\boldsymbol{\zeta}_i(t)\right]\left(\frac{1}{2}\|\boldsymbol{\zeta}_i(t)\|^2-\frac{3}{2}T\right)$$
$$+\sum_i i\mathbf{k}\cdot\boldsymbol{\zeta}_i(t)\left(\frac{1}{2}\|\boldsymbol{\zeta}_i(t)\|^2-\frac{5}{2}T\right)+o(\mathbf{k}), \tag{4.29}$$

and, by taking into account equation (4.24) we observe that, apart from the diffusive terms, hydrodynamical equations for the lattice gas model have exactly the same form as equations for the ideal non-interacting gas with the integration in the expressions for transport coefficients replaced by the trapezoid approximation. One verifies that the cross-correlation of the terms proportional to $\left[\boldsymbol{\xi}_i(t+1)-\boldsymbol{\xi}_i(t)-\boldsymbol{\zeta}_i\right]$ and corresponding to different times vanishes and, thus, the matrix of force auto-correlation functions has the diagonal form. It is convenient to rewrite the momentum force as a sum of two terms; the term parallel to $\mathbf{k}$ and the perpendicular term which defines the shear viscosity coefficient.

$$f^{\mu}_{\mathbf{k}}(t) = \sum_i\left(\boldsymbol{\zeta}^{\perp}_i(t)i\mathbf{k}\cdot\boldsymbol{\zeta}_i+i\mathbf{k}\left[\boldsymbol{\zeta}^{\parallel}_i(t)^2-\frac{1}{3}\|\boldsymbol{\zeta}_i(t)\|^2\right]\right)+o(\mathbf{k}),$$

where $\boldsymbol{\zeta}^{\parallel}_i$ and $\boldsymbol{\zeta}^{\perp}_i$ are the parallel and perpendicular components of the velocity, respectively and in the above expression we average over the random jumps.

Algebraic manipulations give the following expression for the linearized hydrodynamic equations:

$$\partial_t \rho_{\mathbf{k}} = -D\|\mathbf{k}\|^2 \rho_k + i\mathbf{k}\cdot\boldsymbol{\mu}_{\mathbf{k}}, \tag{4.30}$$

$$\partial_t \boldsymbol{\mu}_{\mathbf{k}} = -D\|\mathbf{k}\|^2 \boldsymbol{\mu}_{\mathbf{k}} + i\mathbf{k}\cdot\left[T\rho_{\mathbf{k}} + \frac{s_{\mathbf{k}}}{c_v}\right] + \tilde{\eta}\left[\mathbf{k}\mathbf{k} - \frac{1}{d}\|\mathbf{k}\|^2\hat{\mathbf{1}}\right] : \frac{\boldsymbol{\mu}_{\mathbf{k}}}{T}, \tag{4.31}$$

$$\partial_t s_{\mathbf{k}} = -D\|\mathbf{k}\|^2 s_{\mathbf{k}} + Ti\mathbf{k}\cdot\boldsymbol{\mu}_{\mathbf{k}} + \tilde{\lambda}\|\mathbf{k}\|^2 \frac{s_{\mathbf{k}}}{c_v T^2} \tag{4.32}$$

The contribution to the bulk viscosity coefficient vanishes because of symmetry reasons; $3\left\langle \zeta_i^{\parallel}(t)^2 \right\rangle = \langle \|\boldsymbol{\zeta}_i(t)\|^2 \rangle$. The transport coefficients are given by the following relations:

$$\tilde{\eta} = \int_0^\infty \sum_{ij} \zeta_{xi}(t)\zeta_{yi}(t)\zeta_{xj}(0)\zeta_{yj}(0) \tag{4.33}$$

$$\tilde{\lambda} = \int_0^\infty \sum_{ij} \left(\frac{1}{2}\|\boldsymbol{\zeta}_i(t)\|^2 - \frac{5}{2}T\right)\boldsymbol{\zeta}_i(t)\cdot\left(\frac{1}{2}\|\boldsymbol{\zeta}_j(0)\|^2 - \frac{5}{2}T\right)\boldsymbol{\zeta}_j(0) \tag{4.34}$$

where the integral sign in the above equation denotes the trapezoid approximation to the integral. The above equations for transport coefficients are identical with the ideal gas expressions for the same quantities.

4.3 Computation of the transport coefficients

As an application of the above formalism we derive expressions for transport coefficients in terms of time-correlation functions. With the use of simple approximations to the relaxation dynamics we obtain analytical expressions for such coefficients.

4.3.1 Self-diffusion coefficient

We illustrate application of the expression (4.23) and obtain an expression for the value of the self-diffusion coefficient. The dynamical variable corresponding to the diffusive relaxation process is

$$\mathbf{a}(\mathbf{r}) = \delta(\mathbf{r} - \mathbf{l}),$$

where $\mathbf{l}$ is the position of the marked particle and $\mathbf{a}$ is a one-component vector. In $\mathbf{k}$-space the dynamical variable is expressed as

$$\mathbf{a}_\mathbf{k} = e^{i\mathbf{k}\cdot\mathbf{l}}. \tag{4.35}$$

The expression for the force (4.20) takes the form:

$$\mathbf{f}_\mathbf{k}(0) = e^{i\mathbf{k}\cdot\mathbf{l}(1)} - \left\langle e^{i\mathbf{k}\cdot[\mathbf{l}(1)-\mathbf{l}(0)]} \right\rangle e^{i\mathbf{k}\cdot\mathbf{l}(0)} = i\mathbf{k}\cdot[\mathbf{l}(1) - \mathbf{l}(0)], \tag{4.36}$$

and the expression for the reversible flux vanishes by the Onsager relation (4.16):

$$\left\langle \mathbf{a}_\mathbf{k}(\mathcal{S}(\Gamma, 1))\mathbf{a}_\mathbf{k}^\dagger(\Gamma) - \mathbf{a}_\mathbf{k}(\Gamma)\mathbf{a}_\mathbf{k}^\dagger(\mathcal{S}(\Gamma, 1)) \right\rangle = \left\langle e^{i\mathbf{k}\cdot[\mathbf{l}(1)-\mathbf{l}(0)]} - e^{i\mathbf{k}\cdot[\mathbf{l}(0)-\mathbf{l}(1)]} \right\rangle \equiv 0.$$

Using relation (4.36) and the expression (4.23) we arrive at the following equation:

$$\partial_t \bar{\mathbf{a}}_\mathbf{k} = -\frac{1}{2}\left\langle (\mathbf{k}\cdot[\mathbf{l}(1) - \mathbf{l}(0)])(\mathbf{k}\cdot[\mathbf{l}(1) - \mathbf{l}(0)]) \right\rangle \bar{\mathbf{a}}_\mathbf{k} - \\ - \sum_{t=1}^{\infty} \left\langle (\mathbf{k}\cdot\mathbf{v}(t))(\mathbf{k}\cdot\mathbf{v}(0)) \right\rangle \bar{\mathbf{a}}_\mathbf{k}, \tag{4.37}$$

where we employed the fact that transitions $\mathbf{l}(0) \to \mathbf{l}(1)$ and $\mathbf{l}(t) \to \mathbf{l}(t+1)$ are uncorrelated. We also omitted terms of order $\mathbf{k}^3$ and higher in the above expression.

When the stationary probability distribution is spherically symmetric equation (4.37) is invariant with respect to rotations of space $\mathbb{R}^d$. Thus setting $\mathbf{k}$ to a fixed value, say e_x, we read off the value of the diffusion coefficient from the equation (4.37):

$$D_s = \frac{1}{2}\langle \kappa_2(v_x)\rangle + \frac{1}{2}\langle v_x(0)v_x(0)\rangle + \sum_{t=1}^{\infty}\langle v_x(t)v_x(0)\rangle\,. \tag{4.38}$$

We compare this expression with the value obtained from the definition of the self-diffusion coefficient as the slope of mean-square displacement:

$$D_s = \lim_{t\to\infty}\frac{\|\mathbf{l}(t)-\mathbf{l}(0)\|^2}{2dt},$$

where d is the space dimension. Using the relation

$$\mathbf{l}(t)-\mathbf{l}(0) = \sum_{\tau=1} t[\mathbf{l}(\tau)-\mathbf{l}(\tau-1)],$$

and invariance of the correlation function with respect to time translation we obtain the following relation:

$$D_s = \lim_{t\to\infty}\frac{1}{dt}\sum_{t=1}^{\infty} t\,\langle \mathbf{v}(t)\mathbf{v}(0)\rangle + \\ + \frac{1}{d}\left[\frac{1}{2}\langle([\mathbf{l}(1)-\mathbf{l}(0)])\cdot[\mathbf{l}(1)-\mathbf{l}(0)]\rangle + \sum_{t=1}^{\infty}\langle \mathbf{v}(t)\mathbf{v}(0)\rangle\right],$$

which, for spherically symmetric equilibrium distributions, has the same value as (4.37) if the velocity auto-correlation decays fast enough.

4.3.2 Viscosity coefficient

Following standard procedure[19] we define the viscosity coefficient from the linearized equation of motion for the transverse component of the current:

$$\frac{\partial}{\partial t}\mathbf{j}_t = \frac{\eta}{\rho}\nabla^2\mathbf{j}_t. \tag{4.39}$$

The transverse component of current satisfies the condition of a non-divergent flow: $\nabla \cdot \mathbf{j}_t = 0$.

From comparison of long-time, long-scale decay of the "stress-stress" time correlation function and the microscopic expression for the same quantity we derive the following expression for the viscosity coefficient:

$$\eta = \lim_{\tau\to\infty} \frac{m^2}{TV}\frac{1}{2\tau}\left\langle \left[\sum_{i=1}^{N} y_i(\tau)v_i^x(\tau) - y_i(0)v_i^x(0)\right]^2 \right\rangle. \tag{4.40}$$

The argument in the average in equation (4.40) may be rewritten as

$$\begin{aligned} &y_i(\tau)v_i^x(\tau) - y_i(0)v_i^x(0) = \\ &\quad = \sum_{t=0}^{\tau-1}\big([y_i(t+1) - y_i(t)]v_i^x(t) + [v_i^x(t+1) - v_i^x(t)]y_i(t+1)\big). \end{aligned} \tag{4.41}$$

We attach the meaning of pre- and post-collision velocities of particle i to the variables $v_i^x(t)$ and $v_i^x(t+1)$. Because of local conservation of momentum, the sum of these terms over all particles vanishes.

Let us introduce the notation:

$$\psi(t) = \left\langle \sum_{i,j} (y_i(t+1) - y_i(t))(y_j(1) - y_j(0))v_i^x(t)v_j^x(0) \right\rangle.$$

Jumps at different times and of different particles are uncorrelated so that we express the above formula in terms of velocity correlations and a diffusion term:

$$\psi(t) = \left\langle \sum_{i,j} v_i^x(t) v_i^y(t) v_j^x(0) v_j^y(0) \right\rangle + N\delta(t) \left\langle \kappa_2(v^y(0)) v^x(0)^2) \right\rangle .$$

Under the assumption that the above auto-correlation function decays in a geometrical progression with rate q, the viscosity is found to be:

$$\eta = \lim_{\tau\to\infty} \frac{m^2}{TV} \frac{1}{2\tau} \left(\tau\psi(0) + \sum_{t=1}^{\tau} 2(\tau - t)\psi(t) \right) = \\ = \frac{m\rho}{T} \left[\frac{1}{2} \left\langle \kappa_2(v^y(0)) \right\rangle T + \frac{T^2}{m^2} \frac{1+q}{2(1-q)} \right] . \quad (4.42)$$

If we further assume that only particles at different nodes are uncorrelated we rewrite $\psi(1)$ as sum over sites with at least one particle collision $s \in \mathbb{S}$:

$$\psi(1) = \sum_{n(s)\neq 0} \langle \mathsf{V}_{xy}(s) \mathsf{V}_{xy}(\mathcal{C}(s)) \rangle .$$

Number of the n-particle collisions in a large system is approximately given by the scaled Poisson distribution:

$$p(n) = \|\mathbb{L}\| \frac{\rho^n}{n!} e^{-\rho},$$

with density ρ defined from the relation $N = \|\mathbb{L}\|\rho$ where N is number of particles.

By averaging over collisions with different numbers of particles we arrive at

the expression:

$$\psi(1) = \frac{N}{\rho}\sum_{n=1}^{\infty}\frac{e^{-\rho}}{n!}\fint_{o\in\mathfrak{R}}\int d\mathbf{V}d\mathbf{W}\prod_{i=1}^{n}\delta(\mathbf{w}_i - \mathsf{V} - o(\mathbf{v}_i - \mathsf{V}))\times$$
$$\times P_n(\mathbf{V})\sum_{j=1}^{n} w_{xj}w_{yj}\sum_{l=1}^{n} v_{xl}v_{yl}, \quad (4.43)$$

where ρ was accounted for by the normalization factor in Maxwellian distribution. We note that computation of $\psi(0)$ from the above formula yields:

$$\psi(0) = \frac{N}{\rho}\frac{e^{-\rho}}{n!}\rho^n n\left\langle \mathbf{v}_x\mathbf{v}_x\mathbf{v}_y\mathbf{v}_y\right\rangle = N\left\langle \mathbf{v}_x\mathbf{v}_x\mathbf{v}_y\mathbf{v}_y\right\rangle = N\frac{T^2}{m^2}.$$

Next we determine the value of $\psi(1)$ for the two collision models with different sets $\mathfrak{R}$ of rotations. When set of rotations coincides with $O(d)$, set of all rotations, we perform integration over $\mathbf{W}$ first with subsequent averaging over $\mathfrak{R}$:

$$I = \fint_{o\in\mathfrak{R}}\int d\mathbf{W}\prod_{i=1}^{n}\delta(\mathbf{w}_i - \mathsf{V} - o(\mathbf{v}_i - \mathsf{V}))\sum_{j=1}^{n} w_{xj}w_{yj} =$$
$$= \fint_{o\in\mathfrak{R}}\sum_{j=1}^{n}\left[\mathsf{V}_x + o(\mathbf{v}_i - \mathsf{V})\big|_x\right]\left[\mathsf{V}_y + o(\mathbf{v}_i - \mathsf{V})\big|_y\right] = n\mathsf{V}_x\mathsf{V}_y. \quad (4.44)$$

The average momentum distribution has a Maxwellian form with the power of exponential $-\frac{\mathsf{M}\mathsf{V}^2}{2T}$, yielding the result for $\psi(1)$:

$$\psi(1) = \frac{N}{\rho}\sum_{n=1}^{\infty}\frac{\rho^n e^{-\rho}}{n!}\left\langle \mathbf{v}_x\mathbf{v}_x\mathbf{v}_y\mathbf{v}_y\right\rangle. \quad (4.45)$$

Carrying out the sum in equation (4.45) we arrive at the expression for the viscosity coefficient:

$$q = \frac{1 - e^{-\rho}}{\rho} \tag{4.46}$$

$$\eta = \rho \left[\frac{1}{2} \langle \kappa_2(v^y(0)) \rangle + \frac{T}{m} \frac{1 + \rho - e^{-\rho}}{2(e^{-\rho} - (1 - \rho))} \right] \tag{4.47}$$

We see that in this model, for moderate values of temperature and density, the viscosity is mainly defined by the second term.

Let us now consider the collision rule where $\mathfrak{R}$ is a set of rotations by $\frac{\pi}{2}$ and $-\frac{\pi}{2}$. As one can easily see under action from $\mathfrak{R}$ the product $v_x v_y$ changes sign. For this collision model formula (4.44) yields:

$$I = \sum\!\!\!\!\!\!\int_{o \in \mathfrak{R}} \sum_{j=1}^{n} \left[\mathsf{V}_x + o(\mathbf{v}_i - \mathsf{V})\big|_x \right] \left[\mathsf{V}_y + o(\mathbf{v}_i - \mathsf{V})\big|_y \right] =$$

$$= \sum\!\!\!\!\!\!\int_{o \in \mathfrak{R}} \sum_{j=1}^{n} \left[-v_{ix} v_{iy} - o\mathbf{v}_i\big|_y o\mathsf{V}\big|_x - o\mathbf{v}_i\big|_x o\mathsf{V}\big|_y \right] =$$

$$= \sum_{j=1}^{n} \left[2\mathsf{n}\mathsf{V}_x \mathsf{V}_y - v_{ix} v_{iy} \right]. \tag{4.48}$$

Further integration with respect to $\mathbf{V}$ yields the values for viscosity coefficient and damping factor q:

$$q = -1 + 2\frac{1 - e^{-\rho}}{\rho}$$

$$\eta = \rho \left[\frac{1}{2} \langle \kappa_2(v^y(0)) \rangle + \frac{T}{m} \frac{1 - e^{-\rho}}{2(e^{-\rho} - (1 - \rho))} \right] \tag{4.49}$$

For this collision model the system displays an interesting behaviour. It reveals a strong negative autocorrelation in the system which possesses only

local interactions. This feature enables us to perform simulations in the physically interesting regime of low kinematic viscosity. In later sections we shall numerically investigate the autocorrelation functions discussed above and comment on the agreement between the theoretical and simulated values.

5. NUMERICAL STUDY OF THE LATTICE GAS MODEL

In this section we discuss numerical experiments on the lattice gas model. The results are separated in two groups. The results of the first group serve to validate the theoretical constructs of the previous sections. In this group we also include computations of the transport coefficients using the formulae of Sec. 4. Applications of the lattice gas model to simulations of fluid dynamics constitute the second category of numerical experiments.

5.1 Equilibrium properties

The theoretical results of the previous section are based on an assumption concerning the nature of the local equilibrium distribution. In Sec. 2.6 we gave a proof that, in the Boltzmann approximation, the probability distribution converges to a Maxwell distribution. In order to ensure that a local probability distribution has the Maxwell form we need to establish some facts on the rate of convergence to the stationary distribution. Theoretical results with such content are very few and usually are difficult to obtain for a general model.[20]

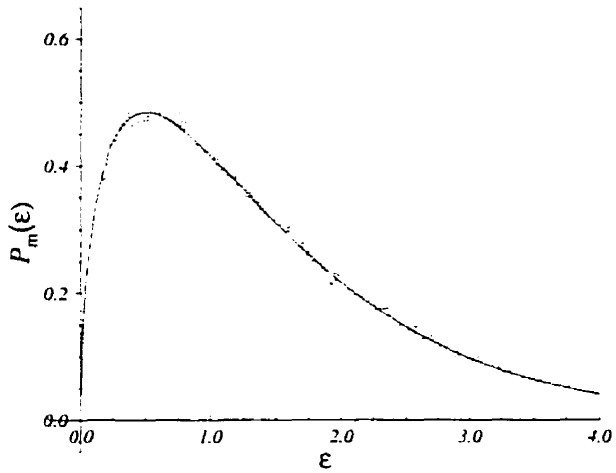

Fig. 5.1 Numerical and theoretical energy probability distribution densities. The solid line shows the Maxwell energy profile. The dotted line is obtained from numerical simulations.

We perform a simulations of the lattice gas model with the following parameters:

$$\rho = 6.0,$$

$$T^* = 1.0,$$

on a cubic lattice with dimensions $40 \times 25 \times 25$ with periodic boundary conditions yielding a total of 1.5×10^5 particles. Initially particles are distributed uniformly in the domain. We assign to the particles initial velocities from the set $\{\pm\sqrt{3}\mathbf{e}_x, \pm\sqrt{3}\mathbf{e}_y, \pm\sqrt{3}\mathbf{e}_z\}$. Thus, the initial energy distribution is

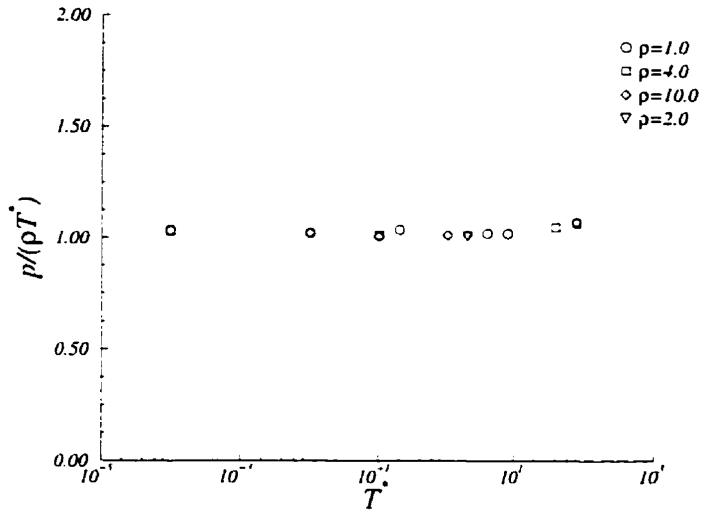

A test of equation of state of the lattice gas model. Fig. 5.2

given by a Dirac function at $\varepsilon = 3/2$ or $P_0(\varepsilon) = \delta(\varepsilon - 3/2)$. We observed that after several steps the energy distribution is thoroughly randomized. The number of steps depends on the system density and is independent of temperature. In general the rate of relaxation to the Maxwell distribution is high and the assumption on the local Gaussian character of the probability distribution holds. In Fig. 5.1 we show the energy probability distribution after 100 automation steps. The solid line represents the Maxwellian energy distribution:

$$P_{\mathrm{m}}(\varepsilon) = \frac{2}{\sqrt{\pi}}\sqrt{\varepsilon}e^{-\varepsilon/T^*}.$$

The dotted line represents the results of numerical simulations. The energy

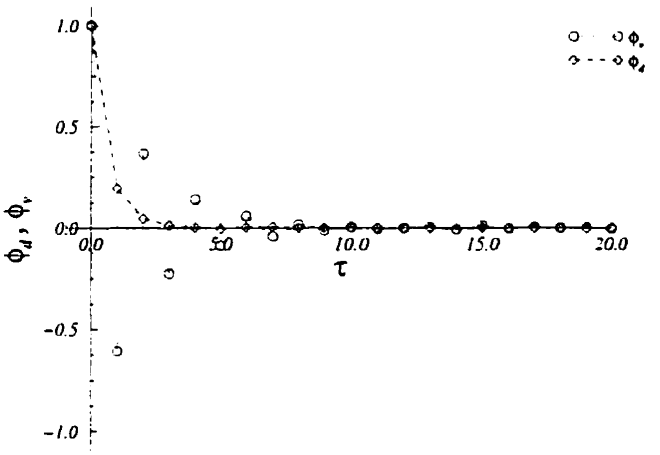

Fig. 5.3 Velocity-velocity and stress-stress normalized time correlation functions for the collision model with an orthogonal scattering of the colliding particles.

segment is divided into 400 bins and probability distribution density for the energy corresponding to the median point of a bin is assigned according to the number of particles in the bin. We found a good agreement between the theoretical prediction and the numerical results. The Maxwell distribution is spherically symmetric and, thus, leads to a symmetric pressure tensor.

The lattice gas model represents a non interacting monatomic lattice gas and its caloric equation of state is simply:

$$U = C_v T.$$

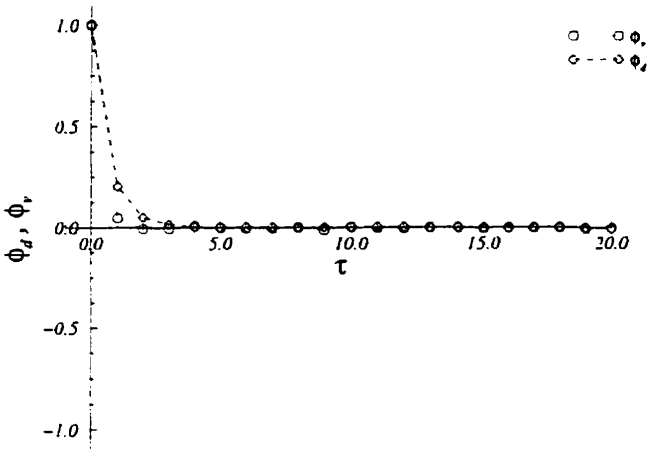

Fig. 5.4 Velocity-velocity and stress-stress normalized time correlation functions for the collision model with a random scattering of the colliding particles.

The second equation of state for the ideal gas is:

$$p = \rho T^*,$$

where ρ is the mass density of a system. We ran a series of simulations on a two dimensional square lattice with dimensions 100×100 for different values of temperature and density. We imposed periodic boundary conditions in one direction and no-slip boundary conditions in the other direction. The no-slip boundary conditions were imposed by inverting the velocity a particle colliding with a wall. The pressure was computed as the total momentum

transferred to a wall during an automation step divided by the wall length. In Fig. 5.2 we present the results of simulations where we observe, as expected for a non-interacting gas, that the ratio $p/(\rho T^*)$ is independent of particle density and is equal to unity for a wide range of temperatures. The deviation from unity for large values of temperatures, when the velocity is comparable with the system linear dimensions, has its origin in the non-Maxwellian properties of the boundary collision rule. The choice of a proper boundary collision kernel is discussed in literature.[21] For moderate values of the temperature this collision rule the system is described by the equation of state of an ideal gas.

For the systems where particles are correlated the Boltzmann approximation breaks down and the results of Sec. 3.1 no longer hold. In this case the results provided by the Green-Kubo formulae are indispensable. In principle, it is possible to obtain values of the transport coefficients by measuring the response of a system to an external field,[22] however, this approach requires a complicated system setup. Application of Green-Kubo formulae yields values of transport coefficients through the computations of time correlation functions. Green-Kubo formulae have been applied to lattice gas models.[23] This approach another advantage is that it provides insight into the dynamics of such time correlation functions and information on the possible contributions to the values of transport coefficients.

In Fig. 5.3 and Fig. 5.4 we present the results of numerical experiments on the

collision models described in Sec. 2.2.3. From the form of equation (4.42), we observe that if the time correlation contribution vanishes the viscosity coefficient is given by the first term of the sum. To reduce the value of the viscosity coefficient we introduced a model with negative stress-stress correlation, which yields a significantly lower value of the viscosity coefficient. In Fig. 5.3 we represent velocity-velocity and stress-stress normalized time correlation functions by dashed and dotted lines, respectively. The simulations were carried out on a square lattice with dimensions 100×100 and parameters:

$$\rho = 5.0,$$

$$T^* = 1.0.$$

We observe that correlations decay in geometrical progression and this is consistent with the Boltzmann approximation. The experimental decay factor, $q = 0.6$, is the same as the theoretical value given by equation (4.49), $q = 0.6$. The corresponding values of the kinematic viscosity are $\nu_{\text{ex}} = 0.1258$ and $\nu_{\text{th}} = 0.1239$ for the experimental and theoretical values of the non-diffusive contribution to the viscosity, respectively. For higher values of density we observe a deviation of experimental values of the damping factor from the theoretical predictions. We attribute this deviation to the development of correlations in the system and a breakdown of the Boltzmann approximation.

In Fig. 5.4 we present the results for the collision model with random scat-

tering. It yields significantly higher values for the viscosity coefficient. For the same parameter values as in Fig. 5.3 we obtained the value of 0.489 for the kinematic viscosity coefficient. The rates of decay of the velocity auto-correlation function are the same for the two models and yeild the same value of the self-diffusion coefficient.

5.2 Simulations of fluid dynamics

In this section we present the results of simulations of the lattice gas model for hydrodynamical flows. Our goal was to determine if the method exibits the turbulent flow characteristics seen in fluid turbulence experiments. The setup of the simulation was chosen for comparison with photographs of a real water flow past cylinder[24] with similar values of the Reynolds number.

In Fig. 5.5 we present the results of simulations of a two dimensional von Karman street[1] using the lattice gas model. The simulations were carried out on a 1200×400 square lattice (5.28×10^6 particles). Parameters of the

[1] Von Karman street is a regime displayed by a flow past cylinder for the range of Reynolds numbers from 70 to 2,500. It is characterised by a system of perodically oscillating wakes past the cylinder.

simulations were:

$$\rho = 11.0,$$

$$T^* = 1.5,$$

$$u_x = 0.5,$$

and for these values of the parameters the system satisfies the condition of validity of Navier-Stokes equation:

$$\frac{u_x^2}{c^2} \ll 1.$$

The value of kinematic shear viscosity for this parameter values in the Boltzmann approximation was found from formula (4.49) and is equal to $\nu = 0.158$.

We impose periodic boundary conditions on the system. We start from a system configuration with uniform particle distribution and zero total momentum. The particles are driven on the system boundary as follows. We assign to all particles with coordinate $x = 0$ velocities from the Maxwell distribution with temperature $T^* = 1.5$ and $u_x = 0.5$. No-slip boundary condition on the object were implemented by inverting velocity of a particle that collided with the object.

The diameter of the circle on the picture is 78 and the value of the Reynolds number is:

$$\mathrm{Re} = \frac{\rho U L}{\eta} = 240,$$

where, conventionally, L is chosen as the circle diameter.

To reduce the statistical noise we averaged the particle distribution over 100 automation steps and a 2×2 cell. For the density used in the simulations we estimate the mean square deviation of the average velocity from the expression for Gaussian random variables: $\langle \delta v^2 \rangle = 3.4 \times 10^{-4}$.

In Fig. 5.5 we present the result of the simulations of von Karman streets. In the figure, a part of the system with dimensions 600×200 is shown and the snapshots correspond to a frames taken each 100 automation steps. A flow on short distances from the object establishes after a transient time, however, a flow tail grows indefinitely until it occupies the entire system length. In experiments with fluid flow for these values of the Reynolds number the existence of von Karman streets is documented[24] (see Figure 4.12.6 of Batchelor G., *An introduction to fluid dynamics*). The density of the fluid is nearly uniform and velocity randomization at the boundary eliminates the feedback due to the periodic boundary conditions in the system.

To investigate a local structure of flow eddies close to the object we performed simulations for a system with a higher Reynolds number. In Fig. 5.6 we present simulations that display the creation of a boundary layer on the surface of the object. The system setup is similar to the one described above with the following parameter values:

$$\rho = 5.0,$$

$$T^* = 1.5,$$

$$u_x = 0.3.$$

The system dimensions are 800×800 and the cylinder diameter $L = 278$. The effective density of the system is higher because the disk occupies approximately 3% of the domain area. The theoretical kinematic shear viscosity and the corresponding Reynolds number are 0.27 and $\mathrm{Re} = 310$, respectively. In this case a small system length prevents the development of the von Karman street and instead a pair of stable vortices forms. However, for this value of the Reynolds number this pair is not stable and a turbulent flow between the cylinder wall and the vortex ensues. In Fig. 5.6 snapshots of the initial stages of the formation of the vortices are shown. The vectors represent the flow field and are colour-coded according to the magnitude of the vertical component of the velocity field. These shapshots are to be compared with the very similar pictures presented in Batchelor G., *An introduction to fluid dynamics*, Fig. 5.11.3.

Since this thesis is not dedicated to the study of the hydrodynamical phenomena but rather to the methods to study such phenomena, further studies of specific hydrodynamic flow problems are not addressed here. However, we note that the fine structure of the small scale eddies as well as large scale structures, existing in the physical systems, are reproduced in the lattice gas model simulations. Thus, we believe that the model can be used to study the behaviour of fluid flow under wide range of conditions. In general, we found the method to be stable with respect to changes of different conditions, the system geometry, temperature and flow velocity.

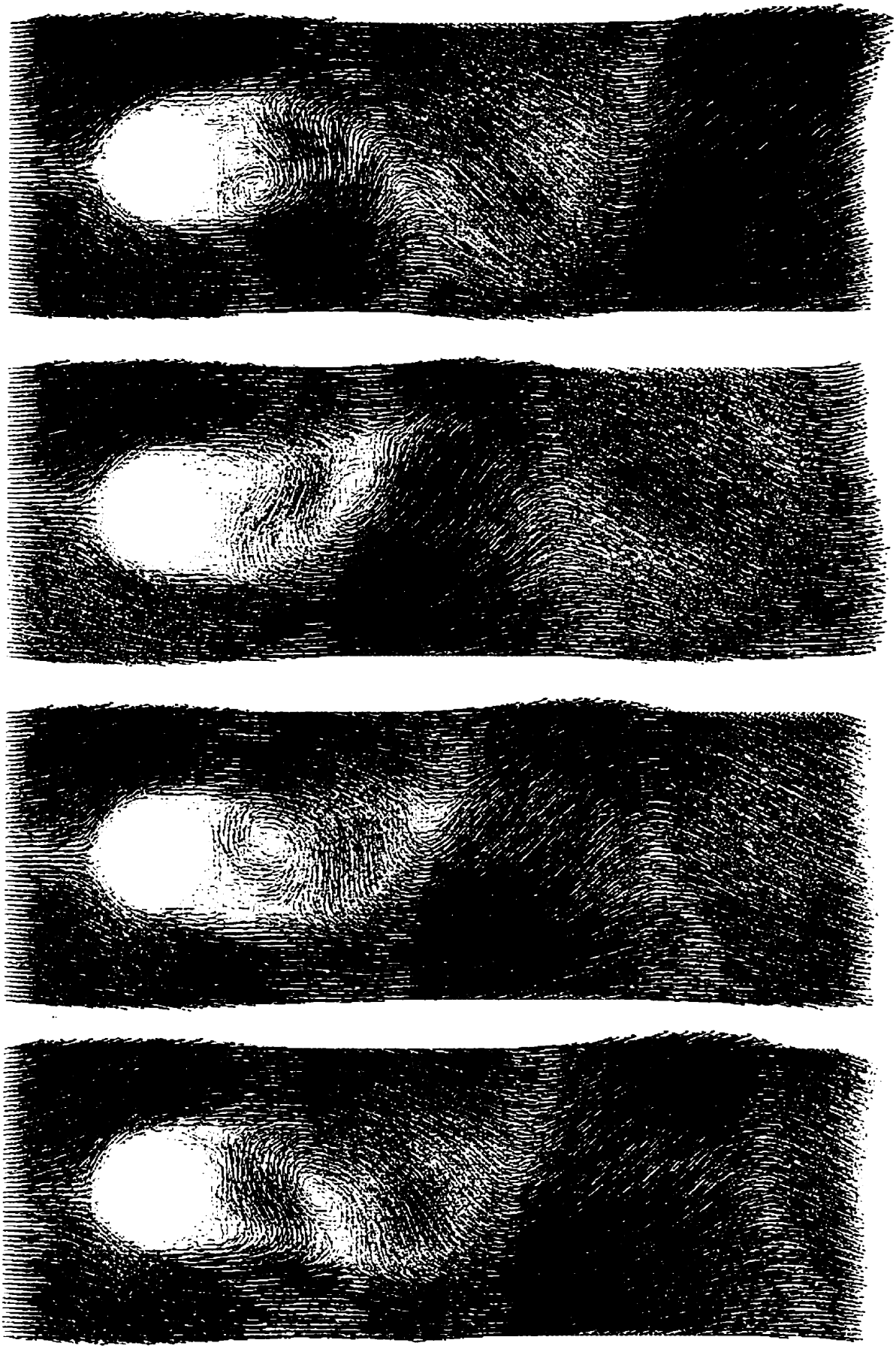

Simulation of two dimensional von Karman street.

Fig. 4

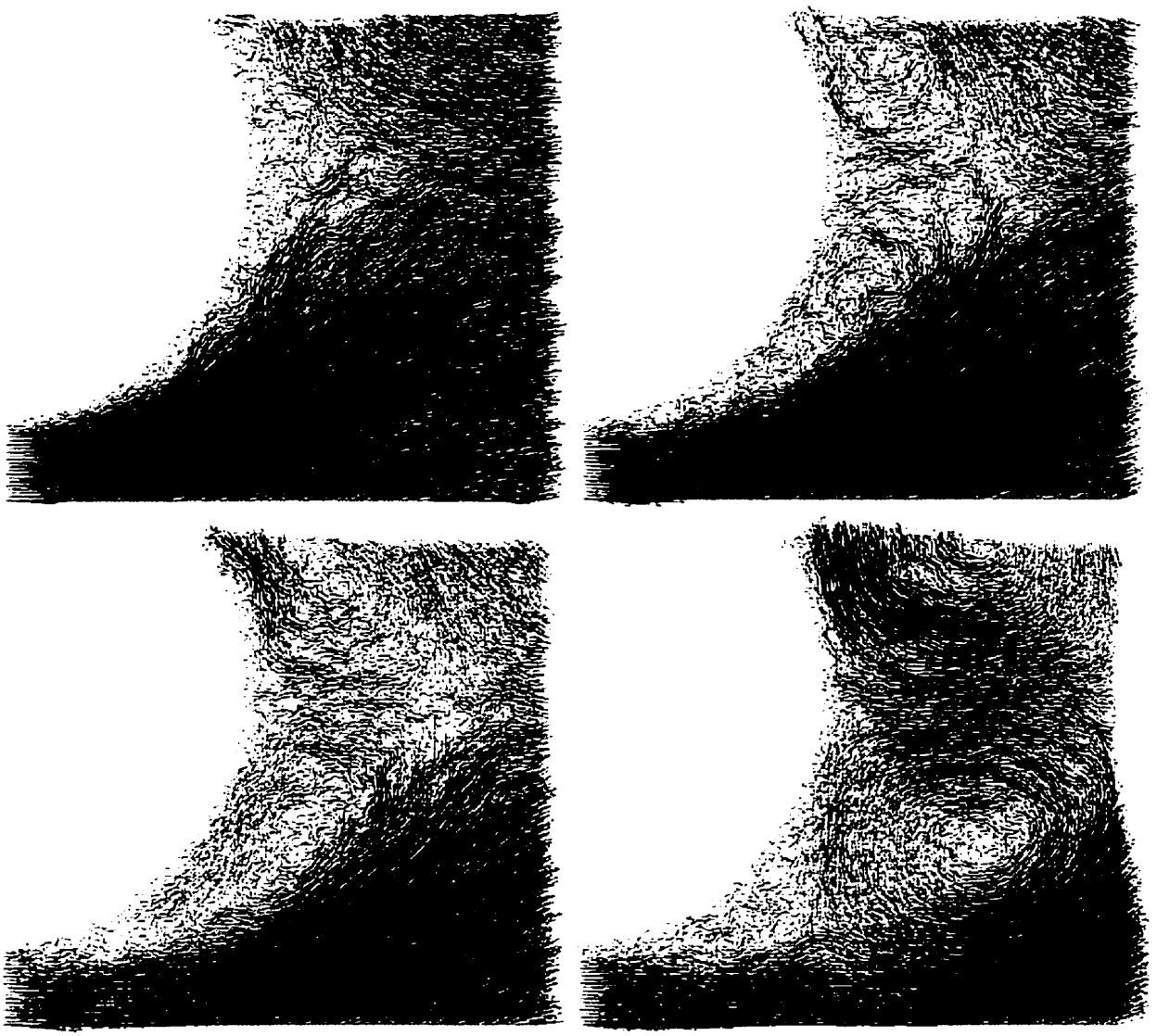

Development of a turbulent boundary layer for a high Reynolds number flow.

Fig. 4.

6. CONCLUSION

The results in this thesis are intended to form a starting point for research on a new class of discrete models for hydrodynamic computations. At the current stage of development spectral methods for solving the Navier-Stokes equation are more efficient than the lattice gas and lattice Boltzmann schemes.[13] The present lattice gas model provides a simple alternative scheme that accounts for the Maxwellian distribution of velocities and is easily extended to treat a wide class of physical and chemical problems. Further studies will determine if the method is competitive with the spectral or other standard simulation methods.

At this point we would like to mention some unsolved problems. An interesting problem is phase separation in multi-component lattice gases. In the traditional lattice gas models phase separation is achieved through the introduction of auxiliary species of particles or through local collision schemes without the semi-detailed balance condition.[8] An implementation of the force through an exchange particle mechanism, which satisfies detailed balance, is a possible approach to this problem and is easily implemented within the context of the present model.

The particle-wall collision scheme requires further investigation. The collision rule used in the present simulations does not adequately describe collisions at high temperatures and, more important, it supports only adiabatically insulated systems.

We believe that the model can also be an efficient tool for the molecular dynamics simulations of reactive fluids or problems where fluctuations are important. We envision applications of such schemes for the modelling of shock waves or combustion fronts. This model can be easily modified to incorporate chemical reactions for which microscopic collision schemes are known.[25] These schemes take into account the excess energy of the reactive binary collisions and satisfy the detailed balance condition. The rates of the reactions obtained in these schemes satisfy the Arrhenius law and have a clear chemical meaning.

We demonstrated the connection between the present model and the evolution of an ideal gas and, on this basis, we believe that the range of applicability of this lattice model is wider than simply the macroscopic Navier-Stokes equations obtained from it on long distance and time scales. In regimes where the system behaviour is unknown or unpredictable the inherent stability of the lattice gas method can be an asset and, we hope, this feature will make this research useful to workers in the field.

BIBLIOGRAPHY

[1] Gary D. Doolen, editor. *Lattice Gas Methods for Partial Differential Equations*, Advanced Research Workshop on Lattice Gas Automata. Addison-Wesley, 1990.

[2] Gary D. Doolen, editor. *Lattice Gas Methods.* MIT/North Holland, 1991.

[3] Jean Pierre Boon, editor. *J. of Stat. Physics*, volume 68(3/4) of *Advanced Research Workshop on Lattice Gas Automata*, New York-London, 1992. Plenum press.

[4] Anna Lawniczak and Raymond Kapral, editors. *Pattern Formation and Lattice-Gas Automata.* Fields Institute Communications. American Mathematical Society, Providence, Rhode Island, 1996.

[5] Uriel Frisch, Brosl Hasslacher, and Yeves Pomeau. Lattice gas automata for the navier-stokes equation. *Phys. Rev. Lett.*, 56(14):1505–1508, 1986.

[6] Norman Margolus. Cam-8: A computer architecture based on cellular automata. In Raymond Kapral and Anna Lawniczak, editors, *Pattern*

Formation and Lattice-Gas Automata, page 165. Fields Institute Communications, AMS, 1996.

[7] A.N. Emerton, P.V. Coveney, and B.M. Boghosian. Lattice-gas simulations of domain growth, saturation, and self-assembly in immiscible fluids and microemulsions. *Phys. Rev. A*, 55(1):708–720, January 1997.

[8] Daniel Rothman and Stephane Zaleski. Lattice-gas models of phase separation: interfaces, phase transitions, and multiphase flow. *Reviews of Modern Physics*, 66(4):1417–1479, October 1994.

[9] Jean Pierre Boon, David Dab, Raymond Kapral, and Anna Lawniczak. Lattice gas automata for reactive systems. *Physics Reports*, 273(2), August 1996.

[10] Renée Gatingnol. Navier-stokes equations for a class of discrete models with different moduli. In Bernie Shizgal and David Weaver, editors, *Rarefied gas dynamics*, page 37. AIAA, 1992.

[11] G. A. Bird. *Molecular gas dynamics*. Oxford University Press, London, 1976.

[12] Guy McNamara and Giunluigi Zanetti. Use of the boltzmann equation to simulate lattice-gas automata. *Phys. Rev. Lett.*, 61(20):2332:2335, 1988.

[13] Shiyi Chen, Zheng Wang, Xiaowen Shan, and Gary D. Doolen. Lattice boltzmann computational fluid dynamics in three dimensions. *J. of Stat. Physics*, 68(3/4):379–400, August 1992.

[14] Uriel Frisch, Dominique d'Humieres, Brosl Hasslacher, Pierre Lallemand, Yves Pomeau, and Jean-Pierre Rivet. Lattice gas hydrodynamics in two and three dimensions. *Complex Systems*, 1:649–707, 1987.

[15] H. Mori. *Prog. Theor. Phys.*, 33:423, 1965.

[16] I. S. Gradshtein and I. M. Ryzhik. *Table of integrals, series and products.* Academic Press, New York, 1965.

[17] Carlo Cercignani. *Mathematical methods in kinetic theory.* Plenum Press, New York, 2 edition, 1990.

[18] R. Kubo. The fluctuation-dissipation theorem. In *Many-Body Problems.* W.A. Benjamin, Inc., 1969. Progress in physics. A reprint series.

[19] Jean Pierre Boon and Sidney Yip. *Molecular hydrodynamics.* McGraw-Hill, New York, 1980.

[20] XXIV Winter School of Theoretical Physics. *Stochastic methods in mathematics and physics.* World Scientific, Singapore, 1989.

[21] Carlo Cercignani. *The Boltzmann equation and its applications*, volume 67 of *Applied mathematical sciences.* Springer-Verlag, New York, 1988.

[22] Leo Kadanoff, Guy McNarama, and Gianluigi Zanetti. A posieuille viscometer for lattice gas automata. *Complex systems*, 1:791–803, 1987.

[23] Jean-Pierre Rivet. Green-kubo formalism for lattice gas hydrodynamics and monte-carlo evaluation of shear viscosities. *Complex systems*, 1:839–851, 1987.

[24] George Keith Batchelor. *An introduction to fluid dynamics*. Cambridge University Press, 1967.

[25] Raymond Kapral. Kinetic theory of chemical reaction in liquids. In I. Prigogine and S. Rice, editors, *Advances in chemical physics*, volume 48. John Wiley & sons, Inc., 1981.

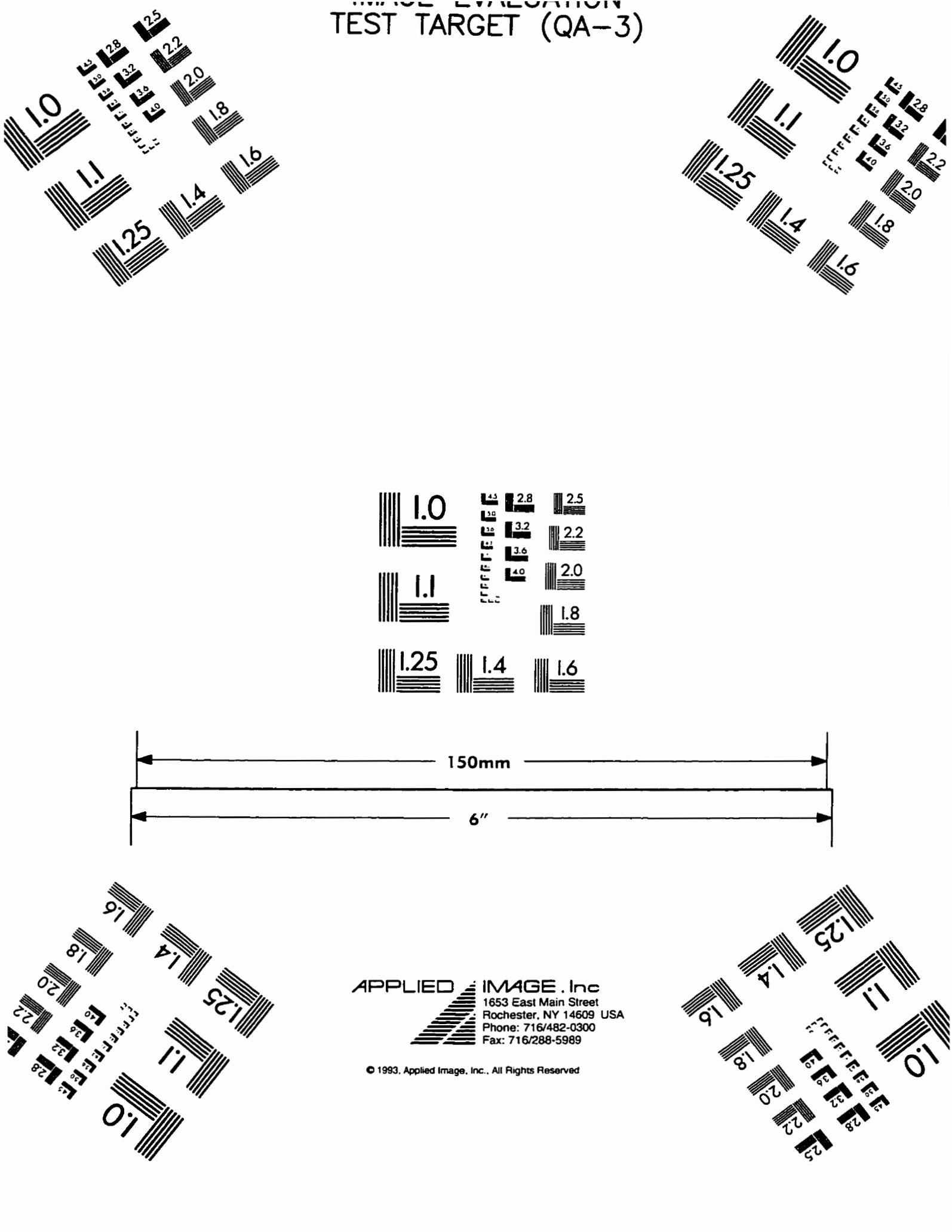
IMAGE EVALUATION
TEST TARGET (QA-3)
1.0
1.1
1.25
1.4
1.6
1.8
2.0
2.2
2.5
2.8
3.2
3.6
4.0
150mm
6"
APPLIED IMAGE, Inc
1653 East Main Street
Rochester, NY 14609 USA
Phone: 716/482-0300
Fax: 716/288-5989
© 1993, Applied Image, Inc., All Rights Reserved